

University of Windsor

Scholarship at UWindor

Electronic Theses and Dissertations

Theses, Dissertations, and Major Papers

7-7-2020

A LabView Based Condition Monitoring Program for a Wind Tunnel Based on Motor Temperature and Fan Vibration

Forhad Reza
University of Windsor

Follow this and additional works at: <https://scholar.uwindsor.ca/etd>

Recommended Citation

Reza, Forhad, "A LabView Based Condition Monitoring Program for a Wind Tunnel Based on Motor Temperature and Fan Vibration" (2020). *Electronic Theses and Dissertations*. 8392.
<https://scholar.uwindsor.ca/etd/8392>

This online database contains the full-text of PhD dissertations and Masters' theses of University of Windsor students from 1954 forward. These documents are made available for personal study and research purposes only, in accordance with the Canadian Copyright Act and the Creative Commons license—CC BY-NC-ND (Attribution, Non-Commercial, No Derivative Works). Under this license, works must always be attributed to the copyright holder (original author), cannot be used for any commercial purposes, and may not be altered. Any other use would require the permission of the copyright holder. Students may inquire about withdrawing their dissertation and/or thesis from this database. For additional inquiries, please contact the repository administrator via email (scholarship@uwindsor.ca) or by telephone at 519-253-3000ext. 3208.

A LabView Based Condition Monitoring Program for a Wind Tunnel Based on Motor Temperature and Fan Vibration

By

Forhad Reza

A Thesis

Submitted to the Faculty of Graduate Studies
through the Department of Mechanical, Automotive & Materials Engineering
in Partial Fulfillment of the Requirements for
the Degree of Master of Applied Science at the
University of Windsor

Windsor, Ontario, Canada

2020

© 2020 Forhad Reza

A LabView Based Condition Monitoring Program for a Wind Tunnel Based on Motor Temperature and Fan Vibration

by

Forhad Reza

APPROVED BY:

X. Chen

Department of Electrical and Computer Engineering

A. Rahimi

Department of Mechanical, Automotive & Materials Engineering

B-A. Schuelke-Leech, Co-Advisor

Department of Mechanical, Automotive & Materials Engineering

J. Defoe, Co-Advisor

Department of Mechanical, Automotive & Materials Engineering

May 14, 2020

Declaration of Originality

I hereby certify that I am the sole author of this thesis and that no part of this thesis has been published or submitted for publication.

I certify that, to the best of my knowledge, my thesis does not infringe upon anyone's copyright nor violate any proprietary rights and that any ideas, techniques, quotations, or any other material from the work of other people included in my thesis, published or otherwise, are fully acknowledged in accordance with the standard referencing practices. Furthermore, to the extent that I have included copyrighted material that surpasses the bounds of fair dealing within the meaning of the Canada Copyright Act, I certify that I have obtained a written permission from the copyright owner(s) to include such material(s) in my thesis and have included copies of such copyright clearances to my appendix.

I declare that this is a true copy of my thesis, including any final revisions, as approved by my thesis committee and the Graduate Studies office, and that this thesis has not been submitted for a higher degree to any other University or Institution.

Abstract

The objective of this research is to create a condition monitoring software program that is able to monitor the operating conditions of the components of an open-loop pusher-style wind tunnel.

The implementation of the condition monitoring program will play an important role to prevent the most unexpected failures as well as performance degradation in wind tunnel components that result from unusual operating conditions such as high temperature and high vibration. To identify the parameters that need to be monitored using the condition monitoring program, fault tree analysis is used. The study finds that wind tunnel failure happens as a result of motor and fan failure. The most likely failure indicators of motor and fan failure are high temperature and high vibration, respectively. To estimate the probability of wind tunnel failure based on motor temperature and fan vibration, a statistical model is developed using the union rule of probability. Furthermore, using the cumulative distribution function of the Beta distribution, the study defines failure probability functions for the motor and fan in terms of operating temperature and vibration, respectively. The condition monitoring program is implemented in LabView software and this research uses simulated data to demonstrate the functionality of the program. The program can perform real-time motor and fan condition monitoring if data acquisition devices are used that are compatible with the LabView software. The user interface of the LabView program displays motor and fan conditions and provides feedback to the wind tunnel user to make appropriate decisions for operation with high motor temperature and/or fan vibration.

Dedication

This thesis is dedicated to my parents Mr. Abul Kalam and Mrs. Bilkis Begum, for their love, support, and sacrifices. I want to give special thanks to my friend Md. Zahirul Hoque for his encouragement and support.

Acknowledgments

I want to express my utmost gratitude to my co-advisors, Dr. Beth Anne Schuelke-Leech and Dr. Jeff Defoe for being excellent mentors. Their mentorship towards the completion of this thesis will help me to make better decisions in my personal and professional life. It has been a great privilege to work with them.

My gratitude also goes to the committee members Dr. Afshin Rahimi and Dr. Xiang Chen, for their insightful advice and effort to review my thesis.

I am also thankful to my friends, especially in the Turbomachinery and Unsteady Flows Research Group.

Contents

Declaration of originality	iii
Abstract	iv
Dedication	v
Acknowledgments	vi
List of Tables	xi
List of Figures	xiii
Nomenclature	xv
1. Introduction	1
1.1 Condition Monitoring	1
1.1.1 Condition Monitoring Methods	2
1.1.2 Importance of Condition Monitoring	3
1.2 Overview of the Open Loop Pusher-Style Wind Tunnel at the University of Windsor ..	4
1.3 Objective and High-Level Approach	6
1.4 Thesis Contributions	7
1.5 Thesis Outline	7
2. Literature Review	9
2.1 Appropriate Technique to Evaluate the Wind Tunnel Failure Modes	9
2.2 Construction of Fault Tree Diagram	11
2.3 Major Causes of the Wind Tunnel Components Failure	13
2.3.1 Major Causes of Electric Motor Failure	13
2.3.2 Major Causes of Fan Failure	17

2.3.3	Major Causes of Inverter Failure	21
2.4	A Review of Statistical Concepts Used in Condition Monitoring	25
3.	Methodology.....	28
3.1	Fault Tree Analysis for the Wind Tunnel.....	28
3.1.1	Fault Tree Analysis for Motor Failure	29
3.1.2	Fault Tree Analysis for Fan Failure	30
3.1.3	Fault Tree Analysis for Inverter Failure	32
3.2	Parameters of Interest.....	33
3.3	Wind Tunnel Failure Model.....	34
3.4	Variables of the Wind Tunnel Failure Model	35
3.5	General Approach of Failure Reference Curve.....	35
3.6	International Standards of Motor Temperature and Fan Vibration.....	36
3.6.1	Motor Temperature	36
3.6.2	Fan Vibration	37
3.7	Assumptions Related to Failure Reference Curves.....	38
3.8	Statistical Concepts Used to Create Failure Reference Curve	40
3.8.1	Cumulative Distribution Function	40
3.8.2	Beta Distribution.....	42
3.9	Determining the Parameters of the Failure Reference Curves.....	43
3.10	Creating the Failure Reference Curves Using CDF of the Beta Distribution	44
3.11	Classification of Motor, Fan, and System Failure.....	46
3.12	Allowable Operating Range for System Failure	48
3.13	Running Average.....	48

4.	Implementation.....	49
4.1	Overview of LabView	49
4.2	Human-Machine Interface Design	49
4.3	Statistical Concepts Used for Data Analysis.....	50
4.3.1	Running Average	50
4.3.2	CDF of the Beta Distribution.....	51
4.3.3	Union Rule of Probability	52
4.4	The Framework of Program Operations.....	52
4.5	Examples of Program Functionality Using Simulated Data	54
4.5.1	Motor Temperature Related Messages	54
4.5.2	Fan Vibration Related Messages	56
4.5.3	Motor Condition Related Information	57
4.5.4	Fan Condition Related Information	58
4.5.5	System Failure Related Information	58
5.	Summary, Contributions, and Future Work	60
5.1	Summary	60
5.2	Thesis Contributions	61
5.3	Conclusion.....	61
5.4	Research Limitations.....	62
5.5	Future Research.....	63
	References	65
	Appendix A Sensitivity Analysis of the Failure Reference Curves	72

Appendix B Determining Shape Parameters (α, β) of CDF of Beta Distribution	81
Appendix C Alpha and Beta Values for Different Optimization Algorithms	84
Appendix D Front Panel and Block Diagram of the Remote Motor Control Program Using LabView	85
Vita Auctoris	86

List of Tables

Table 2.1:Percentage of motor failure [15].	13
Table 2.2: Motor failed components based on the survey [15].	14
Table 2.3: Causes of motor components failure [16].	15
Table 2.4: Failure modes and failure patterns for motor components [17].	16
Table 2.5: Summary of causes of motor failure [15]–[17].	17
Table 2.6: Root causes of centrifugal fan failure [18].	18
Table 2.7: Causes of fan cooling fan failure by failure category [19].	19
Table 2.8: Common causes of centrifugal fan failure [20].	20
Table 2.9: Summary of causes of centrifugal fan failure [18]–[20].	21
Table 2.10: Percentage of tickets issued for inverter components failure [21].	22
Table 2.11: Causes of inverter failure listed in the TECO-Westinghouse inverter manual [22].	23
Table 2.12: Percentage of inverter failure symptoms [26].	24
Table 2.13: Summary of the inverter failure-related information [20] and [21].	24
Table 3.1: Motor faults distribution [30].	30
Table 3.2: F-class motor temperature ratings [39] and [40].	37
Table 3.3: ISO 10816-1 standard for vibration [42].	38
Table 3.4: Classification based on the probability of failure.	46
Table 3.5: Temperature and vibration values for each class.	46
Table 4.1: Number of running average points used for different classes.	51
Table A.1: Temperature classes when prob. is 1% at 40°C or 45°C or 50°C.	73

Table A.2: Temperature classes when prob. is 0.5% or 1% or 1.5% at 45°C	74
Table A.3: Temperature classes when prob. is 75% or 80% or 85% at 150°C	75
Table A.4: Temperature classes when prob. is 80% at 147.5°C or 150°C or 152.5°C.....	76
Table A.5: Vibration classes when prob. is 1% at 1.6 mm/s, 1.8 mm/s, and 2 mm/s.....	77
Table A.6: Vibration classes when prob. is 0.5% or 1% or 1.5% at 1.8 mm/s.....	78
Table A.7: Vibration classes when prob. is 75% or 80% or 85% at 6.5 mm/s.....	79
Table A.8: Vibration classes when prob. is 80% at 6.3 mm/s, 6.5 mm/s and 6.7 mm/s.....	80

List of Figures

Figure 1-1: Open loop pusher-style wind tunnel at the Center for Engineering Innovation	5
Figure 1-2: Components of the open loop pusher-style wind tunnel (a) AC Motor (b) Inverter and (c) Centrifugal Fan.....	5
Figure 1-3: Schematic diagram of the wind tunnel components setup.	6
Figure 2-1: Events and gates used in FTA. (a) Basic event (b) Intermediate event (c) AND gate and (d) OR gate.....	11
Figure 2-2: Example of a fault tree diagram.	12
Figure 3-1: Fault tree diagram for the wind tunnel.....	28
Figure 3-2: Fault tree diagram for motor failure.....	30
Figure 3-3: Fault tree diagram for fan failure.	31
Figure 3-4: Fault tree diagram for inverter failure.....	32
Figure 3-5: FTA representing the early warning signs for the wind tunnel components failure..	33
Figure 3-6: Normal operating temperature of the motor.	38
Figure 3-7: The shape of the failure reference curve is concave up.	40
Figure 3-8: Cumulative distribution function curve.	41
Figure 3-9: The shape of the Beta distribution CDF curve varies for different α and β values....	43
Figure 3-10: Failure reference curve for motor failure.....	45
Figure 3-11: Failure reference curve for fan failure.	45
Figure 3-12: Graphical representation of the temperature classes.....	47
Figure 3-13: Graphical representation of the vibration classes.	47
Figure 3-14: Example of running average.	48

Figure 4-1: Human-machine user interface.	50
Figure 4-2: Flowchart of the LabView program.....	53
Figure 4-3: Front panel marked with segments.	54
Figure 4-4: Temperature related messages. (a) Normal class, (b) Moderate class, (c) High class, and (d) When the temperature difference between actual reading and previous running average reading is higher than 5°C.	55
Figure 4-5: Vibration related messages. (a) Normal class, (b) Moderate class, (c) High class, and (d) When the vibration difference between actual reading and previous running average reading is higher than 1mm/s.....	56
Figure 4-6: Motor condition related information. (a) Motor temperature reading, and (b) Probability of motor failure reading.	57
Figure 4-7: Fan vibration-related information. (a) Fan vibration reading, and (b) Probability of fan failure reading.	58
Figure 4-8: Information related to system failure. (a) Message for the allowable probability of failure, (b) Message for the high probability of failure, and (c) Probability of system failure.....	59
Figure A-1: Probability is 1% at 40°C or 45°C or 50°C and 80% at 150°C	73
Figure A-2: Probability is 0.5% or 1% or 1.5% at 45°C and 80% at 150°C	74
Figure A-3: Probability is 1% at 45°C and 75% or 80% or 85% at 150°C	75
Figure A-4: Probability is 1% at 45°C and 80% at 147.5°C or 150°C or 152.5°C	76
Figure A-5: Prob. is 1% at 1.6 mm/s, 1.8 mm/s, and 2 mm/s and 80% at 6.5 mm/s.....	77
Figure A-6: Prob. is 0.5% or 1% or 1.5% at 1.8 mm/s and 80% at 6.5 mm/s	78
Figure A-7: Prob. is 1% at 1.8 mm/s and 75% or 80% or 85% at 6.5 mm/s	79
Figure A-8: Prob. is 1% at 1.8 mm/s and 80% at 6.3 mm/s, 6.5 mm/s and 6.7 mm/s.....	80

Nomenclature

Symbols

a location parameter of the Beta distribution

b scale parameter of the Beta distribution

$f(t)$ probability density function

$F(x)$ cumulative distribution function

F_f fan failure

M_f motor failure

S_f system failure or, wind tunnel failure

x real number

X random variable

α, β shape parameters of the Beta distribution

Subscripts

f failure

Abbreviations

CDF Cumulative Distribution Function

FMEA Failure Mode and Effect Analysis

FTA Fault Tree Analysis

PHA Preliminary Hazard Analysis

RMS Root Mean Square

1.Introduction

This chapter presents an overview of this research study. At first, the chapter gives a general description of condition monitoring. Then the chapter introduces the wind tunnel that is used for this research. Next, the objectives and thesis contributions are presented. Finally, the structure of this thesis is outlined.

1.1 Condition Monitoring

Condition monitoring is defined as the process of monitoring and determining the condition of a machine while it is operating [1]. A comprehensive condition monitoring program provides thorough diagnostic information to the machine operator. By utilizing condition monitoring, the machine's user will know the working state of the machine. As a result, it is possible to estimate how long a machine can operate in its current state and schedule future repair and maintenance work to avoid failure. The rapid development in sensors and data acquisition technologies have enabled an immense opportunity for condition monitoring. To determine the condition of a machine, different types of parameters such as temperature, vibration, lubrication, etc. are monitored [2]. By evaluating these parameters, the machine condition can be examined either continuously or periodically. The parameters that need to be studied depends on various factors, such as the specific machine design and application [3].

Ming has discussed the evolution of condition monitoring from 1960 to 2000 in [4]. Within this period condition monitoring went through four major development stages because of the advancement in the computer, microprocessor, and software program. In the early 60s,

condition monitoring was mostly dependent on skillful and experienced personnel. Analog instrument-based condition monitoring was introduced in the early 1970s. During this time, heavyweight analog instruments were used to collect condition monitoring data, and mainframe computers were used to store data in magnetic tapes. Digital instrument-based condition monitoring began in the mid-1980s and the instruments used in this period were lightweight with increased accuracy and efficiency. Software-based condition monitoring became available in the mid-1990s. Since then, using software has become popular to perform condition monitoring processes and data analysis.

1.1.1 Condition Monitoring Methods

In [5] and [6], condition monitoring methods are categorized into two different types, off-line monitoring, and online monitoring. For the off-line monitoring method, the machine is taken out of service to inspect the condition and mostly used for scheduled maintenance or routine monitoring. Usually, diagnostic tests and data collection are performed manually in the off-line monitoring methods. On the other hand, for the online monitoring methods, signals of the machine parameters are monitored continuously using wired or wireless systems. The main advantage of the online condition monitoring method is that usually, machine shutdown is not necessary, parameters are monitored without interrupting the machine's normal operation. Examples of the off-line monitoring techniques are insulation resistance inspection and sugar test etc. and the online monitoring techniques are vibration analysis, temperature analysis, current analysis, etc. [5].

In addition to off-line and online methods, Zachrison [7] has classified condition monitoring into model-based and data data-driven approaches. The main idea of model-based approaches is to predict an output signal by analyzing an input signal that passes through a

model. Using a simulation or mathematical model it is possible to detect any unusual condition in the input signal. Examples of model-based approaches are parameter estimation, Kalman filter, parity space, etc. The common practice of data-driven approaches is to compare new data with the preprocessed old data instead of creating a new model. The processes of data comparison and storage vary for individual data-driven approach. Examples of data-driven approaches are Bayesian networks, principal component analysis, etc. These data-driven models are trained with a training sample that includes healthy and faulty data, and the effectiveness of these models depends on the training sample size [8].

1.1.2 Importance of Condition Monitoring

Condition monitoring provides a myriad of benefits. The benefits that are relevant for this project are listed as follows.

- Condition monitoring increases machine reliability and operational lifetime because it helps to find potential failure at an early stage. As the monitoring parameter provides valuable information about machine condition, condition monitoring assists to identify imminent failure before a complete failure happens. The knowledge about imminent failure helps the machine operator to take appropriate actions that result in increased machine reliability and operational lifetime.
- In most cases, it is a proactive monitoring process that identifies any abnormality in a system or machine at the time of its occurrence. Usually, an abnormality is detected if the monitoring parameter values vary from the normal operating values.
- In most instances, condition monitoring analyzes the health condition, so it can be used not to operate a machine in a state when a machine has severe performance degradation.

For instance, if a machine's performance degradation occurs towards the maximum limit of a parameter such as temperature or vibration, using condition monitoring it is possible to operate the machine within the parameter's limit when the possibility of performance degradation is low.

- Condition monitoring helps to avoid secondary damage because it can detect a failure before the primary failure leads to a secondary failure. For instance, deterioration of a motor's bearing can cause total bearing failure and bearing failure might lead to rotor failure [9].

1.2 Overview of the Open Loop Pusher-Style Wind Tunnel at the University of Windsor

The focus of this research is the open loop pusher-style wind tunnel at the Center for Engineering Innovation (CEI), at the University of Windsor. The active components of the wind tunnel are motor, fan, and inverter. The wind tunnel is depicted in Figure 1-1 and the components are shown in Figure 1-2. To represent the wind tunnel components setup, a schematic diagram is shown in Figure 1-3. The motor and inverter used for the wind tunnel are from TECO-Westinghouse Inc. The AC motor can output a maximum of 100 horsepower and it can rotate at a maximum speed of 3,600 RPM. The input voltage for the inverter is 575V. The fan installed at the wind tunnel is a centrifugal fan and it is from Northern Blower. Currently, the wind tunnel does not have a condition monitoring program to monitor the components. So, a condition monitoring program is needed that will help to identify incipient failures as well as deterioration of performance of the wind tunnel components.



Figure 1-1: Open loop pusher-style wind tunnel at the Center for Engineering Innovation (CEI), at the University of Windsor.



a)



b)



c)

Figure 1-2: Components of the open loop pusher-style wind tunnel (a) AC Motor (b) Inverter and (c) Centrifugal Fan.

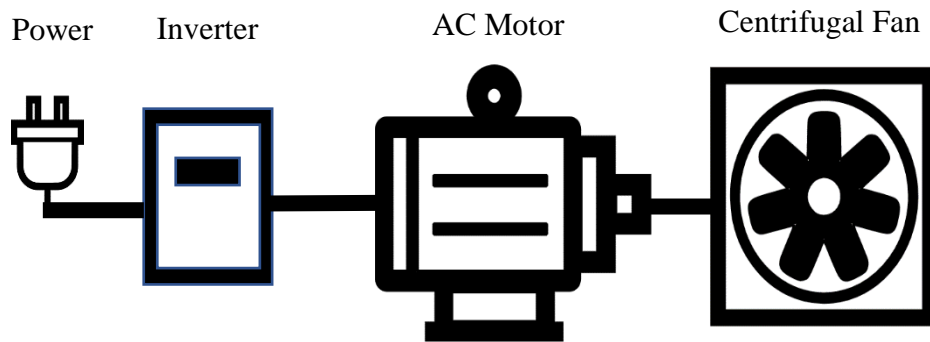


Figure 1-3: Schematic diagram of the wind tunnel components setup.

1.3 Objective and High-Level Approach

This thesis aims to create a condition monitoring software program for the wind tunnel.

The program will utilize a model based on the addition rule of probability to determine the failure probability of the wind tunnel. The program will also use cumulative distribution function to analyze the parameters of the wind tunnel components. The program will be able to perform real-time monitoring about the state of the wind tunnel components when appropriate hardware such as data acquisition devices and sensors will be used. Furthermore, the program will give real-time feedback using text warnings and visual indications based on the operating state of the components. To create the condition monitoring program, the research also focuses on the following tasks.

1. Identify the appropriate failure analysis technique to evaluate the failure modes. This will help to identify the failure modes as well as root causes of the wind tunnel and its components.

2. Investigate the most likely root causes of the wind tunnel components failure. This will determine the parameters that need to be monitored using the program.
3. Identify the normal operating range of the components at which probabilities of component failures are low.

1.4 Thesis Contributions

The major contribution of this thesis is that it presents a condition monitoring program to prevent wind tunnel components failure. The program has the ability to analyze input signals using the statistical concept cumulative distribution function of the Beta distribution. This thesis also contributes to the area of failure analysis of the wind tunnel components. The thesis includes the major root causes of the wind tunnel components failure. Furthermore, using the failure analysis technique this research finds the parameters that need to be monitored by the condition monitoring program.

1.5 Thesis Outline

Chapter 2 presents a thorough literature review on the wind tunnel components failure. The chapter also focuses on identifying a failure analysis technique to outline the major causes of wind tunnel failure. Following this, chapter 3 includes fault tree diagrams for the wind tunnel components and introduces a probability-based model. The chapter also focuses on determining the variables of the model. A LabView software-based condition monitoring program is presented in chapter 4. Using simulated data, a detailed description of the program operations is

also included in this chapter. Conclusion, research limitations and future work are discussed in chapter 5.

2. Literature Review

This chapter investigates the literature review articles related to motor, fan, and inverter failures. Furthermore, this chapter includes basic information about failure analysis techniques as well as statistical concepts that are used in condition monitoring.

2.1 Appropriate Technique to Evaluate the Wind Tunnel Failure Modes

First and foremost, before developing the condition monitoring program, this research has to find the root causes that lead to the wind tunnel failure and identify the parameters that need to be monitored using the condition monitoring program. To figure out the root causes of the wind tunnel components a failure analysis technique is needed that will have the combinations of failure modes for each component. There are several techniques to determine the failure modes of a component such as fault tree analysis (FTA), preliminary hazard analysis (PHA), failure mode and effect analysis (FMEA), and process mapping.

Reay [10] has described the FTA as a top-down deductive technique that starts with a top event and develops downwards to map the causes of a program failure. In other words, the FTA visualizes the combinations of failures that cause a program failure. Two types of analysis can be performed using FTA, qualitative, and quantitative. Qualitative FTA is used to identify the combinations of events that will lead to the program failure and the purpose of quantitative FTA is to determine the probability of a program failure. The main advantage of FTA is that it graphically shows the logical sequences of a failure. The disadvantage of FTA is that the tree diagram becomes extremely large for a complex system.

According to Sharma and Srivastava [11], the FMEA is used to identify potential failures including their causes and effects from a system, process, design, and/or service. The analysis evaluates and prioritizes the risks associated with the failures. It also suggests actions that can reduce or eliminate potential failures from occurring. Each failure mode is rated with a risk priority number that is calculated based on severity, occurrence, and detection of the failure. The risk priority number helps to identify the failures that have high-risk. As a result, appropriate actions can be taken to reduce or eliminate high-risk failures. The drawback of FMEA is that high-risk failures might be ignored because of inaccurate risk priority numbers.

Gould et. al [12] have mentioned that the PHA is used to identify all potential hazards during the design and development of a process or an event. The main purpose of PHA is not to control the hazards but to recognize the hazards. The advantages of the analysis are that it ranks the identified hazardous events based on their severity and proposes follow-up actions and additional safety measures to prevent any accident. The disadvantage of PHA is that it might not identify all the hazards because the analysis is performed before the completion of a process or an event.

Phillips and Simmonds [13] have stated that process mapping is a visual and impartial way to identify problems and how the problems may be solved. In other words, process mapping represents a series of steps or actions that help to achieve an outcome. It uses flowcharts to illustrate the tasks and flow of a process. This helps to identify the problems involved in a process. One of the main disadvantages of process mapping is that it allows to include insignificant and unnecessary steps of a process.

For this research, FTA will be used to evaluate the wind tunnel failure modes because it graphically outlines the combinations of the failures of the wind tunnel using the root causes of

the component's failures. FTA will also help to identify the parameters for the condition monitoring program. The main reasons other methods are unsuitable for this research are because they do not solely focus on failure modes and provide redundant information that this research does not intend to use.

2.2 Construction of Fault Tree Diagram

In the FTA, the main failure event of interest is known as a top event [14]. A fault tree diagram is created using events and gates. The gates and events used in this thesis are shown in Figure 2-1. The events are either intermediate or basic, and they are used to map the failure causes of the top event. The intermediate events can be further developed to find failure causes; however, basic events can not be developed further. Intermediate and basic events are represented by rectangles and circles, respectively.

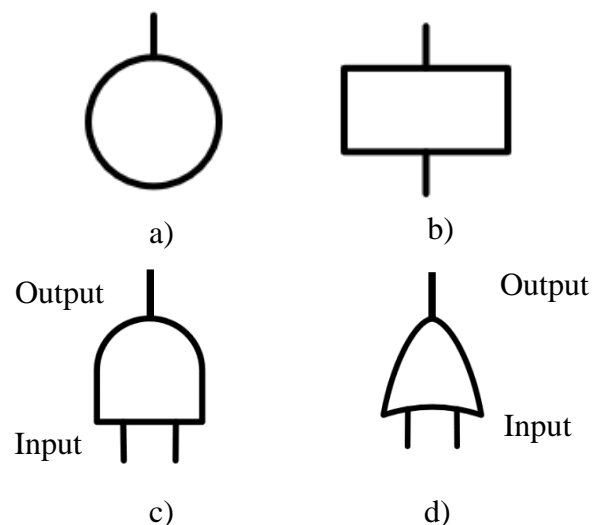


Figure 2-1: Events and gates used in FTA. (a) Basic event (b) Intermediate event (c) AND gate and (d) OR gate.

The gates are used to create a relationship between the events. In this thesis, two types of gates are used: AND gate and OR gate. The functionalities of the fault tree AND gate and OR gate are the same as Boolean intersection and union operations. For the AND gate, if all the input events occur at the same time, then the output event will occur. For the OR gate, the event will occur if at least one input event occurs.

The example provided in Figure 2-2 represents a qualitative fault tree diagram. The fault tree diagram has six basic events (1, 2, 3, 4, 5, and 6), three intermediate events (A, B, and C), three OR gates, and one AND gate. Starting with the top event, System Failure is connected to an output of an OR gate that has three inputs. System Failure will happen if one of the intermediate events occurs. The intermediate events A and C are connected to the outputs of OR gates, so events A and C will take place if one of their corresponding basic events occurs. The intermediate event B is connected to an AND gate that has two inputs. So, event B will happen if both inputs occur.

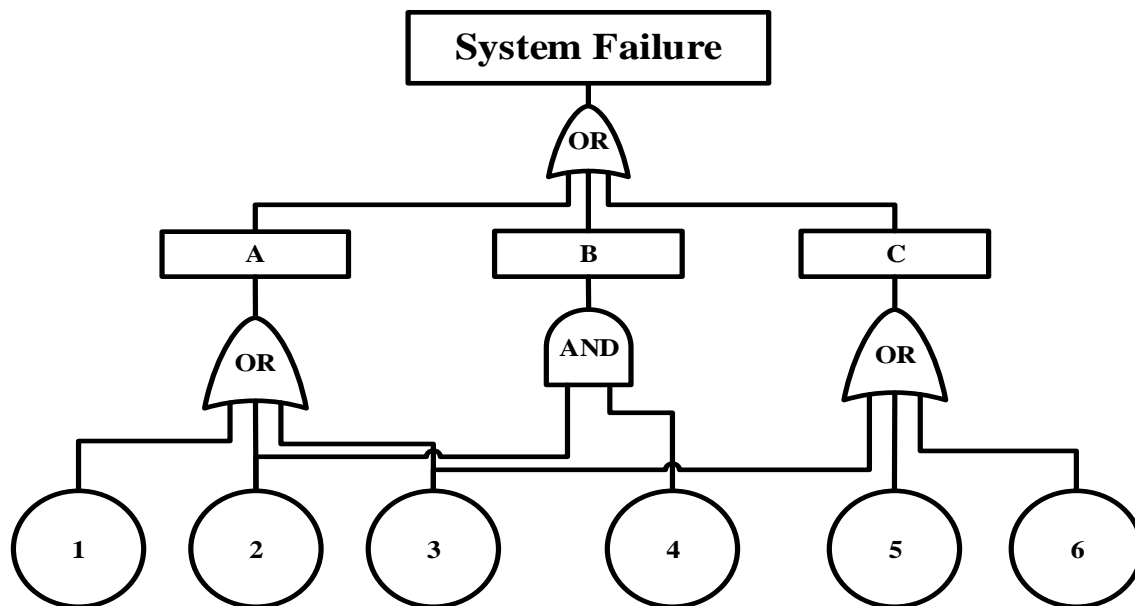


Figure 2-2: Example of a fault tree diagram.

2.3 Major Causes of the Wind Tunnel Components Failure

Although there are enormous number of factors that contribute to motor, fan, and inverter failures, this thesis focuses on the major root causes that give early warning signs of failures. In the following sections, articles are discussed that include the common root causes of motor, fan, and inverter failures.

2.3.1 Major Causes of Electric Motor Failure

O'Donnell et al. [15] have performed an electric motor reliability analysis from a survey where a total of 1,141 AC and DC motors were used and the survey found 360 cases of motor failure. Even though both AC and DC motors are used in the survey, this reliability analysis is important for the research because it includes information about the most likely causes of motor failure. Table 2.1 shows the list of causes of motor failure and it is observed that mechanical crack, insulation breakdown, and overheating are the primary causes of motor failure. The study also finds that bearing and winding are the most failed components than any other components, as shown in Table 2.2.

Table 2.1:Percentage of motor failure [15].

Causes of Failures	Number of failures
Mechanical crack	113
Overheating	45
Insulation breakdown	42
Electrical fault or malfunction	26
Transient overvoltage	5
Stalled motor	3
Others	107

Table 2.2: Motor failed components based on the survey [15].

Failed Component*	Induction Motors
Bearing	152
Winding	75
Rotor	8
Shaft or CPLG	19
External device	10
Not Specified	40
*Some motors have more than one failed component per motor failure.	

Badawi and Almuahini [16] have proposed a reliability model for electric motor driven (EMD) systems where they have analyzed the failure modes of motor components using over 100 EMD systems. They have designed a fault tree model to identify the causes of failures in EMD systems. The main root causes that are found in the fault tree model are shown in Table 2.3. The authors have categorized the root causes into five categories: environmental stress, thermal stress, mechanical and dynamic stress, electromagnetic stress, and other stresses. They have found that bearing, winding, and shaft are the three main components that contribute to motor failures and they have concluded that 80% of the motor failures are related to bearing failures. As seen in Table 2.3, the temperature has a high effect on bearing that gives an idea that the temperature is one of the early warning signs for motor failure.

Table 2.3: Causes of motor components failure [16].

	Shaft	Bearing	Stator	Rotor
Environmental Stress	<ul style="list-style-type: none"> • Corrosion • Moisture • Erosion 	<ul style="list-style-type: none"> • Excessive ambient temperature 	<ul style="list-style-type: none"> • Chemical • Excessive ambient temperature 	<ul style="list-style-type: none"> • Contamination • Excessive ambient temperature
Thermal Stress	<ul style="list-style-type: none"> • Temperature gradients • Rotor bowing 	<ul style="list-style-type: none"> • Friction • Lubricant • Ambient temperature 	<ul style="list-style-type: none"> • Thermal aging • Loading • Ambient temperature 	<ul style="list-style-type: none"> • Thermal overload & unbalanced
Electromagnetic Stress	<ul style="list-style-type: none"> • Sideload • Out of phase reclosing 	<ul style="list-style-type: none"> • Electrostatic coupling 	<ul style="list-style-type: none"> • Dielectric aging • Corona • Transients 	<ul style="list-style-type: none"> • Noise • Circling currents
Mechanical and Dynamic Stress	<ul style="list-style-type: none"> • Torsional load • Axial load 	<ul style="list-style-type: none"> • Misalignment • Shaft/Housing fits 	<ul style="list-style-type: none"> • Coil movement • Rotor strikes 	<ul style="list-style-type: none"> • Fatigue • Material deviations
Other Stresses	<ul style="list-style-type: none"> • Manufacturing process 	<ul style="list-style-type: none"> • Vibration and shock 	<ul style="list-style-type: none"> • Air gap 	<ul style="list-style-type: none"> • Wrong rotation direction

Bonnet [17] has introduced a methodology to diagnose the root causes of a failed motor. The proposed methodology uses a checklist of failure modes and failure patterns. The methodology also includes lists of questions that are related to the failed motor's appearance, application, and maintenance history. The checklist is based on stresses associated with motor components such as stator, rotor, bearing, and shaft. The checklist groups failure modes and failure pattern according to each motor component, as shown in Table 2.4. The checklist is useful for this thesis because it includes information about the parameters that are responsible for the motor component's failure.

Table 2.4: Failure modes and failure patterns for motor components [17].

Motor Component	Failure Mode/Class	Failure Pattern
Stator Winding	Turn to turn Phase to phase Coil to coil Open circuit	Symmetrical Single phased Non-symmetrical and grounded Non-symmetrical and no ground
Rotor Assembly	Shaft Bearing Lamination Squirrel cage	Thermal Magnetic Mechanical Environmental
Ball bearings	Fatigue spalling Wear Lubrication failure Cracks Seizures	Thermal Vibration and noise Lubricant quality Mounting Mechanical & electrical damage
Shaft	Overload Fatigue Corrosion	Ductile Beach marks Shear lips

Table 2.5 shows a summary of the causes of motor failure. The purpose of this table is to find the common failure modes that are presented in the previous references. The table also helps to understand the failure types and their corresponding failure causes. The table categorizes the failure causes in terms of mechanical failure, electrical failure, environmental conditions, and human error. It is noticed from the table that most of the causes are related to mechanical failure. The causes of mechanical failure are categorized according to the failure of the mechanical parts. The table also shows that bearing has more causes of failure compared to other mechanical parts.

Table 2.5: Summary of causes of motor failure [15]–[17].

Failure Type		Causes
Mechanical failure	Bearing	<ul style="list-style-type: none"> • Fatigue • Wear • Lubrication failure • Friction • Misalignment • Crack
	Shaft	<ul style="list-style-type: none"> • Overload • Fatigue
	Stator	<ul style="list-style-type: none"> • Coil movement • Rotor strikes
	Rotor	<ul style="list-style-type: none"> • Incorrect shaft/ Core fit • Fatigue/ Part breakage • Poor rotor to stator geometry
Electrical failure		<ul style="list-style-type: none"> • Overcurrent • Overvoltage
Environmental conditions		<ul style="list-style-type: none"> • High ambient temperature • Corrosion • Moisture • Erosion
Human error		<ul style="list-style-type: none"> • Overload (high RPM) • Frequent start/ stop

2.3.2 Major Causes of Fan Failure

In [18] a thorough list of centrifugal fan failure problems and their associated root causes are listed, as shown in Table 2.6. The table shows that overheated bearings, overload on the driver, high vibration, and high noise levels related problems have the most root causes. It is also noticed that high vibration has more root causes than other problems. This literature review article has great importance for this research because the article includes almost all the root causes associated with centrifugal fan failure. The article also helps to understand the problems that occur because of those root causes.

Table 2.6: Root causes of centrifugal fan failure [18].

THE CAUSES	THE PROBLEM									
	Insufficient Discharge Pressure	Intermittent Operation	Insufficient Capacity	Overheated Bearings	Short Bearing Life	Overload on Driver	High Vibration	High Noise Levels	Power Demand Excessive	Motor Trips
Abnormal End Thrust				•			•			
Aerodynamic Instability		•	•	•	•		•	•		
Air Leaks in System	•	•	•				•			
Bearings Improperly Lubricated						•		•		•
Bent Shaft				•	•	•	•		•	
Broken or Loose Bolts or Setscrews				•			•			
Damaged Wheel	•		•	•						
Dampers or Variable-Inlet Not Adjusted	•		•							
Dirt in Bearings				•			•			
Excessive Belt Tension				•			•			•
External Radiated Heat				•						
Fan Delivering More Than Rated Capacity						•	•			
Fan Wheel or Driver Imbalanced				•			•			
Foreign Material in Fan Causing Imbalance				•			•	•		
Incorrect Direction of Rotation	•		•			•	•			
Insufficient Belt Tension							•	•		
Misalignment of Bearings, Coupling, Wheel				•		•	•	•	•	
Motor Improperly Wired						•	•	•		•
Packing Too Tight or Defective Stuffing Box						•	•		•	•
Specific Gravity or Density Above Design						•	•		•	
Speed Too High		•		•	•	•	•			•
Speed Too Low	•	•	•					•		•
Too Much Grease in Ball Bearings				•						
Total System Head Greater Than Design	•		•	•		•			•	
Total System Head Less Than Design		•					•			•
Unstable Foundation		•		•			•	•		
Vibration Transmitted to Fan from Outside				•			•	•		
Wheel Binding on Fan Housing				•		•	•	•		•
Worn Bearings							•	•		
120-Cycle Magnetic Hum							•	•		
• Common Failure Modes of Centrifugal Fans										

Although a centrifugal fan is used for the wind tunnel, this thesis discusses a literature review article that is based on a cooling fan because the article presents an actual fan failure analysis on 33 samples [19]. Table 2.7 shows the results obtained from the failure analysis. The table includes the failure category and the failure causes associated with each category. The study finds that most cooling fan failures are related to mechanical failure, electrical failure, and fan installation. This article is helpful for the research because it categorizes the root causes as well as organizes the root causes in rank order.

Table 2.7: Causes of fan cooling fan failure by failure category [19].

Fan Failure Category	Failure Causes (in rank order)	Number of Failures
Mechanical failure	<ul style="list-style-type: none"> • Bearing failure • Thermal distortion • Impeller stress cracking 	8
Electrical failure	<ul style="list-style-type: none"> • Electric overstress • PCB cracking damage to components • Wiring errors 	8
Fan installation	<ul style="list-style-type: none"> • Connector crimping or pin opens • Reversed airflow • Loose cabling • Excessive thermal resistance 	8
Acoustic failure	<ul style="list-style-type: none"> • Nominal fan noise creates customer satisfaction issues • Fan blade interference 	5
Serviceability	<ul style="list-style-type: none"> • Poor access raises service costs 	3
System cooling performance	<ul style="list-style-type: none"> • Overheating of tape drives 	1

Table 2.8 shows the list of troubleshooting processes that are obtained from the Greenheck centrifugal fan user manual [20]. The manual includes an extensive list of problems and causes that are related to the centrifugal fan. From the list, this thesis sorts out the common problems that are also found in other literature review articles. Table 2.8 shows that excessive noise, temperature, and vibration are common problems and they are caused by various factors

such as defective bearing, insufficient lubrication, misalignment of the shaft, motor, etc. This user manual categorizes the root causes in terms of parameters. This is useful for this research because it helps to understand parameters that show the early warning signs of fan failure.

Table 2.8: Common causes of centrifugal fan failure [20].

Problem	Causes	Corrective Action
Excessive Noise	Wheel rubbing	Adjust wheel. Tighten the wheel hub or bearing.
	Bearings	Replace defective bearing(s). Lubricate bearings.
	Wheel unbalance	Clean all dirt off the bike. Check wheel balance.
Overheated Shaft Bearing	Lubrication	Check for excessive or insufficient grease in the bearings.
	Mechanical	Replace damaged bearing. Relieve excessive belt tension. Align bearings. Check for the bent shaft.
Excessive Vibration	Belts	Adjust the tightness of belts. Replacement belts should be a matched set.
	System unbalance	Check alignment of the shaft, motor, and pulleys. Check wheel balance, rebalance if necessary.
	Coupling	Check alignment between coupling, motor, and fan shafts.

Table 2.9 shows the summary of the causes of centrifugal fan failure and lists the problems associated with the causes. The listed problems are related to vibration, temperature, noise, and overload. It is observed from the table that several failure causes contribute to vibration, temperature, and noise related problems. The table also shows that most of the failure causes lead to vibration-related problems.

Table 2.9: Summary of causes of centrifugal fan failure [18]–[20].

Causes	Problems			
	Vibration related	Temperature related	Noise related	Overload
Mechanical parts failure	•	•	•	
Vibration transmitted from outside	•	•	•	
Aerodynamic instability	•	•	•	
Unstable foundation	•	•	•	
Misalign bearing, coupling	•	•	•	
Improper lubrication	•	•	•	
Broken/ loose bolts/ screws	•			
Fan wheel imbalanced	•			
Air leaks	•			
High RPM				•
Bent shaft				•
Incorrect rotating direction				•

2.3.3 Major Causes of Inverter Failure

Golnas [21] has analyzed the inverter components failure based on 3,500 service tickets issued by SunEdison’s Renewables Operation Center. The service tickets were used to keep records of issues related to power plant components such as inverter, meter, AC Subsystem, etc. The study finds that the highest percentage of tickets, 43% were issued for inverter related failure. Table 2.10 shows the percentage of tickets issued for different inverter components failure. It is noticed that 28% of the inverter failed because of software failure and other major components of inverter failure are AC contactor and inverter board. The reason this study is important for this research is that it gives thorough information about the inverter failure areas that are obtained from a large sample size. It is inferred from the study that software-related failure is the primary root cause of inverter failure.

Table 2.10: Percentage of tickets issued for inverter components failure [21].

Failure Area	Percent of tickets
Control Software	28%
Card/Board	13%
AC Contactor	12%
Fan(s)	6%
Matrix/IGBT	6%
Power Supply	5%
AC Fuses	4%
DC Contactor	4%
Surge protection	3%
GFI Components	3%
Capacitors	3%
Internal Fuses	3%
Internal Relay/Switch	3%
DC Input Fuses	2%
[additional fields]	5%

The user manual of the installed TECO-Westinghouse inverter includes a list of probable faults and warnings [22]. From the manual, this thesis sorts out the faults that lead to potential inverter failure, as shown in Table 2.11. The faults listed in the table are also found in the literature review articles [23] and [24]. Table 2.11 shows that the most likely root causes for inverter failure are related to voltage, current, temperature, and communication error. This user manual is important for this research because it includes the list of causes of inverter failure and their appropriate solutions.

Table 2.11: Causes of inverter failure listed in the TECO-Westinghouse inverter manual [22].

LED display	Description	Cause	Possible solutions
Overvoltage	Voltage exceeds level.	The voltage is too high.	<ul style="list-style-type: none"> • Reduce the input voltage. • Replace braking transistor
Under voltage	Voltage is low.	The voltage is too low.	<ul style="list-style-type: none"> • Replace control board or complete inverter.
Heatsink overheat	The temperature is too high.	<ul style="list-style-type: none"> • Ambient temp. too high. • Cooling fan failed 	<ul style="list-style-type: none"> • Replace the cooling fan. • Reduce load / Measure output current
Inverter overload	Inverter thermal protection tripped.	Load too heavy.	Reduce motor load, check the duty cycle.
Communication error	LCD keypad communication error.	Keypad and inverter are unable to communicate.	Replace control board
Inverter over heating	Inverter overheats warning.	Digital input overheats warning active.	<ul style="list-style-type: none"> • The multi-function input function set incorrectly. • Check to wire
Overcurrent	The current reaches a high level.	<ul style="list-style-type: none"> • Inverter current too high. 	<ul style="list-style-type: none"> • Check load and duty cycle operation.

Avor and Chang [25] have performed a reliability analysis for variable frequency drive using FMEA. Their FMEA model includes several failure modes for an inverter. The top failure modes listed in the model are insulated gate bipolar transistor not switching, clamp capacitor failure, and gate unit supply failure. In [23] inverter failures are found because of fuse failure, stress, damage, or aging of parts such as a switch, capacitor, and fan.

Estratios et al. [26] have investigated the inverter faults and failure based on 295 inverter cases. Table 2.12 shows the inverter failure symptoms that they observed from the study. The table shows that 33% of the inverter failed because of voltage malfunction. Other common failure symptoms of inverter failure are display malfunction and test procedure or firmware update.

Table 2.12: Percentage of inverter failure symptoms [26].

Failure Symptoms	Percentage (%)
Output Voltage Malfunction	33
Test Procedure/ Firmware update	30
Display Malfunction	27
Cooling System Malfunction	5
Failure Indication on Display	5
Other malfunction	4

Table 2.13 shows a summary of the inverter failure-related information utilizing the knowledge learned from previous references. The table includes failure types and their corresponding failure causes or areas. The table categorizes the failure types into electrical failure, hardware failure, and software failure.

Table 2.13: Summary of the inverter failure-related information [20] and [21].

Failure Type	Failure Cause / Area
Electrical failure	<ul style="list-style-type: none"> • Overvoltage • Under voltage • Overcurrent
Hardware failure	<ul style="list-style-type: none"> • Fan(s) • Display malfunction • LCD keypad failure • Capacitors, Card/Board • AC/ DC Contactor • AC/ DC Fuses • Internal Fuses • Surge protection • Matrix/IGBT • Internal Relay/Switch • GFI Components • Wire
Software failure	<ul style="list-style-type: none"> • Control Software • Communication protocol failure • Firmware update

2.4 A Review of Statistical Concepts Used in Condition Monitoring

Currently, a wide range of statistical concepts, machine learning algorithms, signal processing techniques, and mathematical functions are used in condition monitoring. This research only focuses on the statistical concepts that are found commonly in the literature. Several statistical concepts, namely Bayes' theorem, hidden Markov model, and time series forecasting are widely used in condition monitoring. A basic description of these concepts is described as follows:

Stone [27] has stated that Bayes' theorem is a probability-based theorem that utilizes the prior information of an event and when new information of that event becomes available, it updates the posterior probability. The posterior probability is a conditional probability that is revised or updated after considering new information. In statistics, conditional probability represents the probability of one event based on its relation to another event. Because of this feature, Bayes' theorem has a wide range of applications in terms of decision making, especially in the fields of science, biology, and medicine, etc. [27]. One of the reasons Bayes' theorem is used in condition monitoring is because the theorem allows for updating failure information about a parameter when new failure data become available. The disadvantage of Bayes' theorem is that the posterior probability is heavily influenced by the prior information. As a result, the theorem can generate misleading results.

Zoubin [28] has defined the hidden Markov model as a tool that represents probability distributions over sequences of observations. The hidden Markov model has two properties. First, the hidden Markov model uses a Markov chain to acquire the transition between variables or states. A Markov chain is a model that gives probabilities of a sequence of random variables

or states. Second, the hidden Markov model assumes that the variables or states are hidden from the observer. The hidden Markov model can be divided into two layers, the hidden layer, and the observation layer. In the hidden layer, the Markov chain exists, and the observation layer is considered as the output of the hidden layer. There are three algorithms of hidden Markov model: forward-backward, Viterbi, and Baum-Welch.

In condition monitoring, the time series forecasting method is used to predict a machine performance using parameter data. Adhikari and Agrawal [29] have defined the time series forecasting as predicting the future by understanding the knowledge from the past. In time series forecasting, past observations are analyzed to develop a mathematical model and future events are predicted using the mathematical model. The mathematical model is generated using the time series method. Time series is defined as a sequential set of data points that are measured over successive times. A time series generally has four components: trend, cyclical, seasonal, and irregular. Seasonal variations of a time series are fluctuations that repeat over a specific period. Trend variations correspond to the up or down movement of fluctuations. Cyclical variations describe the medium-term changes in a time series. Irregular variations are caused by unpredictable influences. Popular time series models used in forecasting are Autoregressive (AR), Moving Average (MA), Autoregressive Moving Average (ARMA), and Autoregressive Integrated Moving Average (ARIMA).

The above-described concepts are not suitable for this research because they have several constraints. The Bayes' theorem possesses variable that relates to the prior probability of an event and the value of the prior probability variable is not always available. Besides, results obtained from the Bayes' theorem do not always satisfy the real-world expectations. The hidden Markov model is not appropriate to evaluate wind tunnel parameters because it requires a

sequence of possible events and the events are dependant on each other based on probability values. The time series forecasting is not suitable for this project because the project intends to create a real-time monitoring program that will monitor the state of the wind tunnel components if data acquisition devices are used.

A comprehensive literature review on the failures of the motor, fan, and inverter, as well as basic descriptions of FTA and several statistical concepts, were summarized in this chapter. Since the purpose of this research is to create a condition monitoring program, so the research has to identify the parameters that need to be monitored using the program. In the next chapter, FTA will be used to find the parameters that show the most obvious signs of failures associated with motor, fan, and inverter. In addition, the next chapter presents a statistical model as well as discusses several statistical concepts that will be used to develop the condition monitoring program.

3. Methodology

This chapter presents FTA to evaluate the failure modes of the wind tunnel. The chapter also includes a statistical model that uses union rule of probability and introduces failure reference curves to determine the variables of the model. In addition, the chapter categorizes the motor temperature and fan vibration values into different classes.

3.1 Fault Tree Analysis for the Wind Tunnel

To graphically represent the combinations of the wind tunnel failures, qualitative FTA is used. A fault tree diagram is created using the failures of the wind tunnel components motor, fan, and inverter, as shown in Figure 3-1. The wind tunnel failure represents the top event of the fault tree diagram and is connected to the output of an OR gate. The component's failures are connected to the inputs of the OR gate. The reason OR gate is used because the wind tunnel failure will happen if one of the components fails.

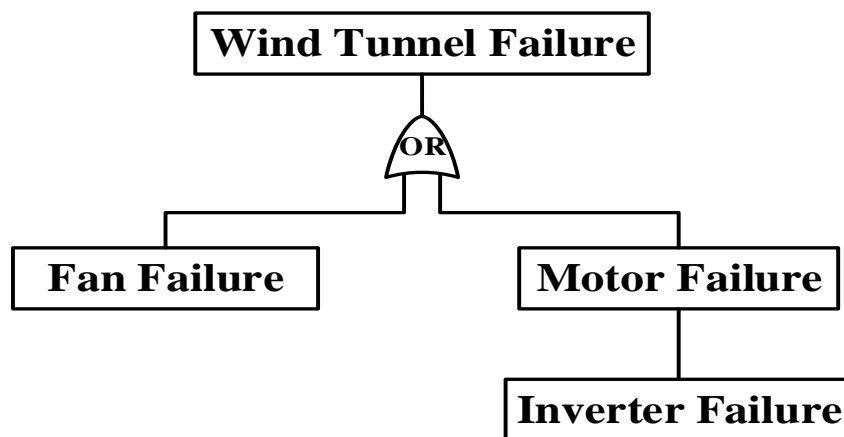


Figure 3-1: Fault tree diagram for the wind tunnel.

To investigate the common failures of the components, manufacturers were contacted. The manufacturers suggested that the most likely causes of the motor, fan, and inverter failures are related to temperature, vibration, and cooling fan failures, respectively. In the following sections, the FTA for the wind tunnel components is presented based on the knowledge learned from the literature review and considering the manufacturer's suggestions.

3.1.1 Fault Tree Analysis for Motor Failure

A fault tree diagram for motor failure is developed, as shown in Figure 3-2. The diagram includes the most likely root causes of the motor failure that are found common in most of the literature review articles. The diagram has several intermediate events such as temperature, vibration, human error, electrical, and mechanical parts failure. The temperature-related failures include the root causes that lead to mechanical parts failure and electrical failure. The diagram shows that the root causes of mechanical parts failure also contribute to vibration-related failures.

Table 3.1 shows the percentage of motor faults based on a survey of 1,005 motors that was done by the Electric Power Research Institute and the faults listed in the table cause 90% of motor failures [30]. The table shows that the percentage of stator faults and rotor faults is 37% and 10%, respectively. In [31] it is found that one of the main causes of stator and rotor faults is overheating. Furthermore, another study shows that 35% - 40% of motor failures are because of the stator winding insulation failure and high temperature is the main reason for insulation failure [32]. Considering the above-mentioned data and the manufacturer's suggestion, it is certain that the temperature is the most likely parameter that shows early warning signs of motor failure.

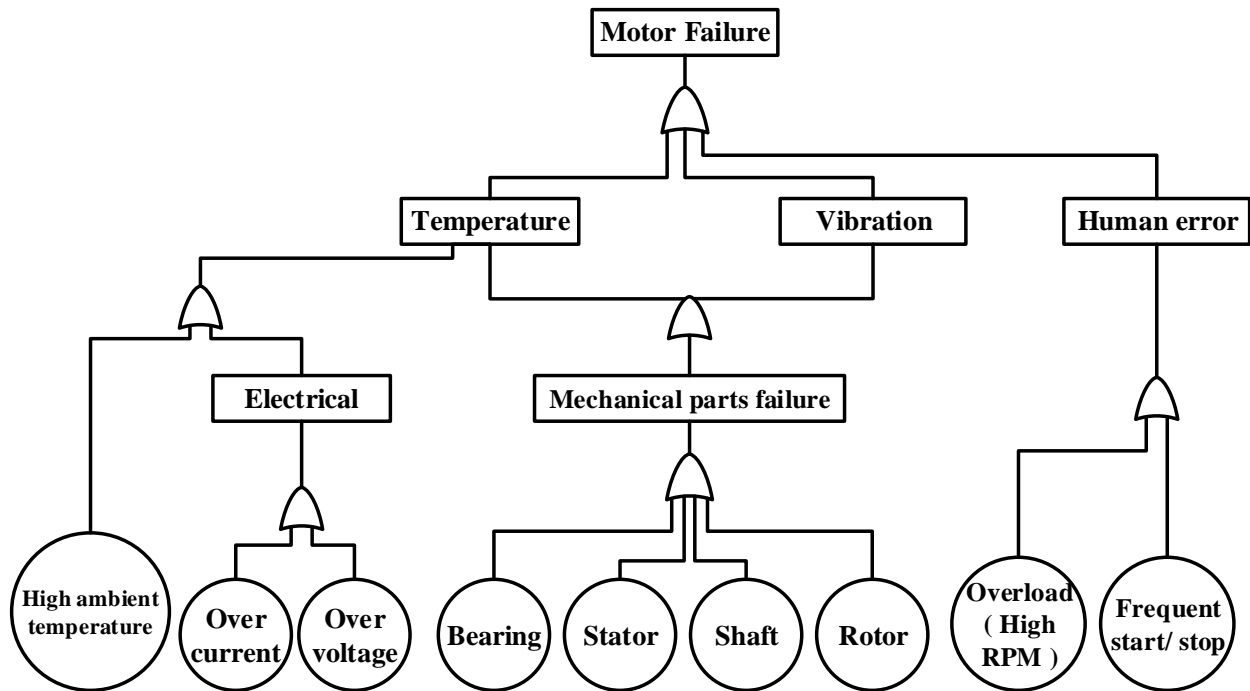


Figure 3-2: Fault tree diagram for motor failure.

Table 3.1: Motor faults distribution [30].

Types of faults	Percentage of Faults
Bearing	41
Stator	37
Rotor cage (broken rotor bars/ end-rings)	10
Air-gap irregularities and others	12

3.1.2 Fault Tree Analysis for Fan Failure

Figure 3-3 shows the fault tree diagram for fan failure. The primary root causes of fan failure are included in the diagram. The intermediate events of the fault tree are vibration, temperature, noise, and overload. The diagram shows that vibration, temperature, and noise share the root causes related to mechanical parts failure, misaligned bearings or coupling, aerodynamic

instability, etc. There are several other root causes such as air leaks, imbalanced fan wheel, and broken/loose screws that also cause vibration.

Hipni et. al [33] investigated the damage analysis of a centrifugal exhaust fan. Their analysis shows that the most dominant damage symptom is noticed in bearing and excessive vibration is the reason for bearing damage. In addition, the centrifugal fan operator's manual from Kice Industries Inc. lists the common problems associated with a centrifugal fan [34]. The primary problems listed in the manual are excessive vibration, inadequate performance, excessive noise, and premature component failure. Incorporating the centrifugal fan failure information and the knowledge learned from the fan fault tree diagram, it is found that the vibration is the primary indicator for centrifugal fan failure.

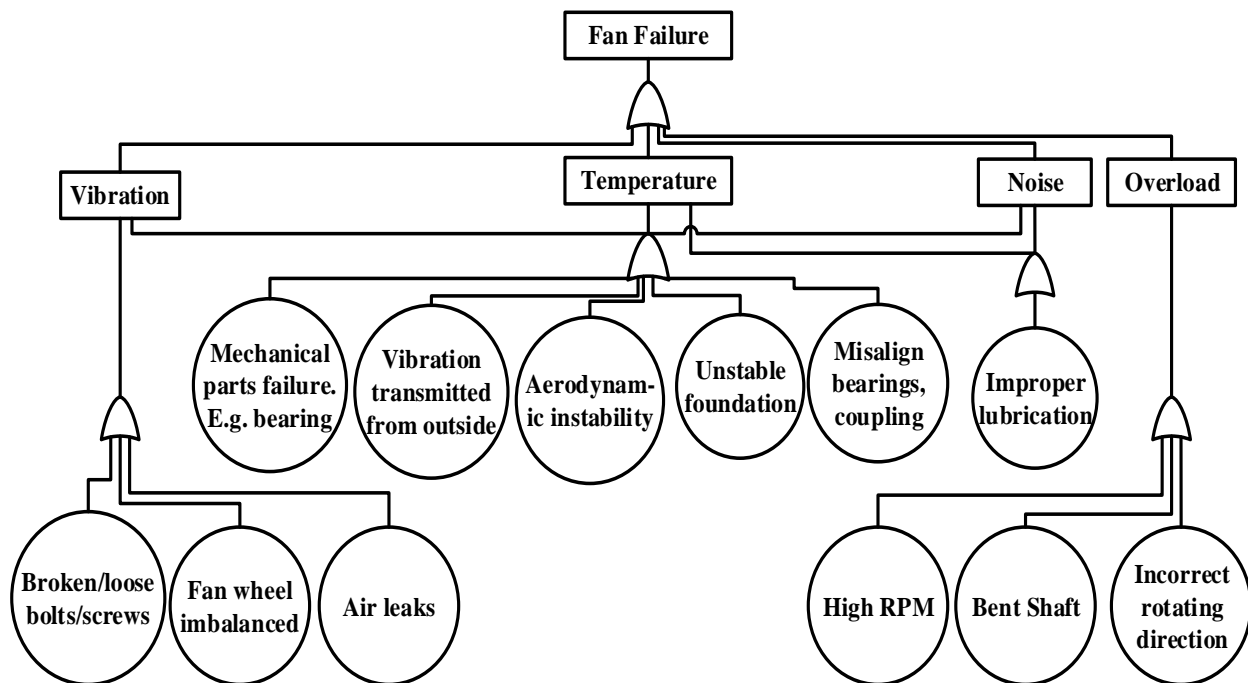


Figure 3-3: Fault tree diagram for fan failure.

3.1.3 Fault Tree Analysis for Inverter Failure

Figure 3-4 represents the fault tree diagram for inverter failure. The diagram helps to understand the failure mechanism of the inverter. The intermediate events of the fault tree diagram are failures related to electrical, hardware, and software. From the diagram, it is found that the two primary reasons for electrical failure are current and voltage. The main root causes of the hardware failure are cable failure, cooling fan failure, and LCD keypad failure. For the cooling fan failure, it is the temperature that leads to hardware failure. From the TECO-Westinghouse user manual, it is found that software failure happens if the inverter's software and keypad on the control board are unable to communicate.

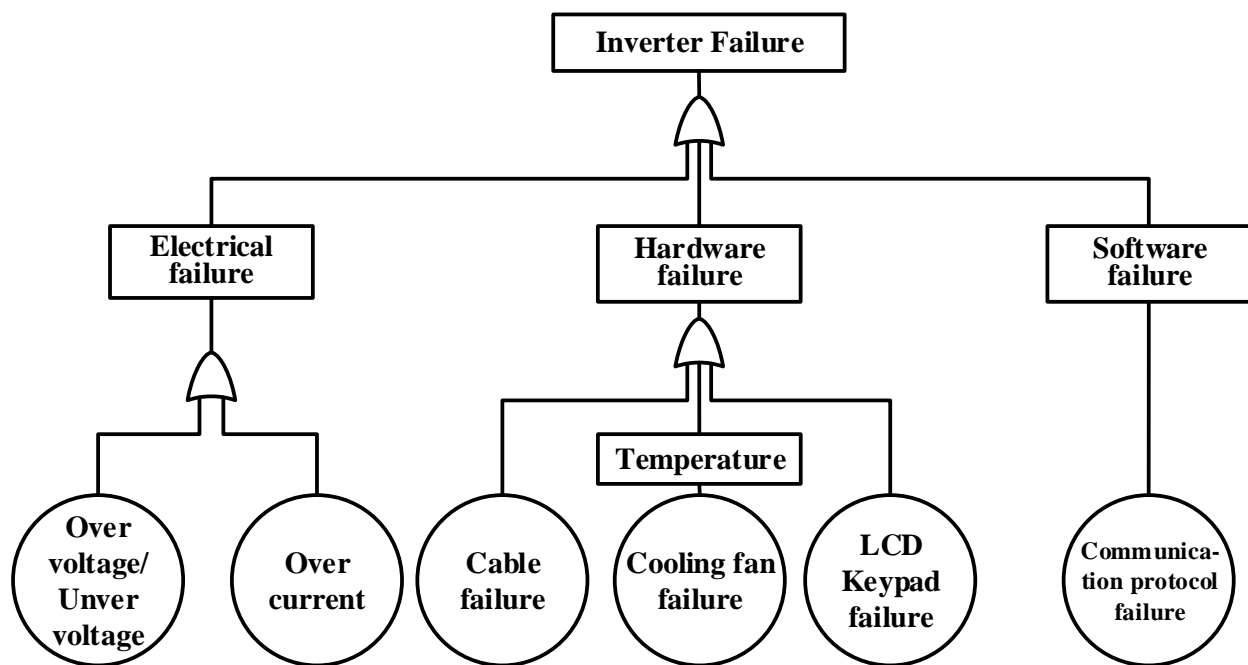


Figure 3-4: Fault tree diagram for inverter failure.

3.2 Parameters of Interest

This research finds the parameters for the condition monitoring program considering the knowledge learned from the FTA of the wind tunnel failure and the manufacturer's suggestion. As temperature and vibration show the early warning signs of motor and fan failure, respectively, they are the primary parameters of interest for this research, as shown in Figure 3-5. This research will not consider inverter failure for the condition monitoring program because Figure 3-1 shows that the inverter failure can cause motor failure, however, it can not cause wind tunnel failure.

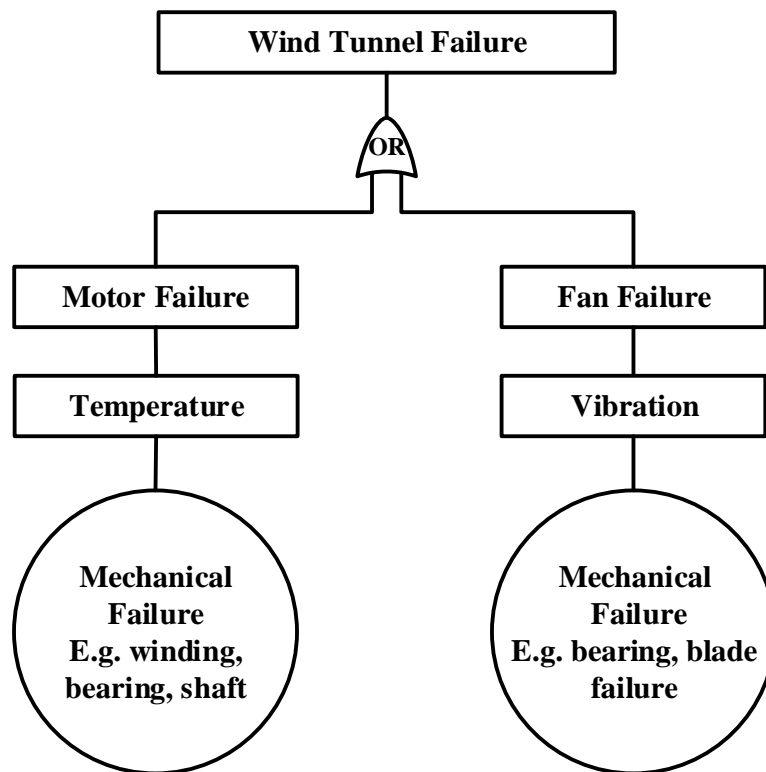


Figure 3-5: FTA representing the early warning signs for the wind tunnel components failure.

3.3 Wind Tunnel Failure Model

To create the wind tunnel failure model, this research uses the union rule of probability because it meets the real-world expectation in terms of wind tunnel failure [35]. For instance, the probability of wind tunnel failure should always be higher than the probability of individual component failure. Furthermore, it is a simple rule to use; the theories described in the literature review chapter are complicated and do not fulfill the appropriate requirements of this project. The equation of the addition rule of probability is shown in Eq. (3-1).

$$P(A + B) = 1 - ((1 - P(A)) * (1 - P(B))) \quad (3-1)$$

The motor temperature and fan vibration are independent variables for this research. The wind tunnel failure model considering the motor temperature and fan vibration is shown in Eq. (3-2).

$$P(S_f) = 1 - ((1 - P(M_f)) * (1 - P(F_f))) \quad (3-2)$$

where, S_f , M_f , and F_f represent system failure, motor failure, and fan failure, respectively. The variables $P(M_f)$, $P(F_f)$, and $P(S_f)$ mean the probability of motor failure, fan failure, and system failure, respectively. For this research, it is considered that temperature is the reason for motor failure and fan failure happens as a result of vibration.

3.4 Variables of the Wind Tunnel Failure Model

In Eq. (3-2), there are two variables, $P(M_f)$ and $P(F_f)$. To get the values of these variables, motor and fan manufacturers were contacted. However, manufacturers did not share the information. So, this thesis presents motor and fan failure reference curves to obtain the variables. The curves represent the characteristics of motor and fan failure and show the relation between temperature and vibration values in terms of the probability of motor and fan failure values. The general idea of creating the failure reference curve is presented in the following section.

3.5 General Approach of Failure Reference Curve

The following steps are taken into consideration when creating the failure reference curve for any parameter.

- Identify the endpoints or scale of the curve. This can be obtained from the maximum and minimum operating range of the parameter. Usually, values of the operating range can be acquired from the manufacturers, international standards, or machine parameter rating.
- Determine the shape of the failure reference curve in terms of failure probability versus the parameter values. For instance, the shape of the curve can be concave up, concave down, or s-shaped.
- Utilize the cumulative distribution function concept to create the failure reference curve.

The cumulative distribution function is calculated from the integral of the probability density function and the probability density function represents the probability distribution of the parameter value [36].

- Utilize the Beta distribution for the cumulative distribution function because Beta distribution allows any type of shape for the cumulative distribution function curve [37].

Detailed descriptions of the cumulative distribution function and Beta distribution are presented in the later sections of this chapter. The shape of the cumulative distribution function curve of the Beta distribution depends on four coefficients, one location parameter, one scale parameter, and two shape parameters [38]. The location parameter and scale parameter are obtained from the endpoints of the curve. To determine the shape parameters, two points are needed that fall under the shape of the curve. The two points are used to create two equations of the cumulative distribution function. Solving the two equations will give the values of shape parameters. Once all the coefficient values are obtained then the failure reference curve can be generated using the cumulative distribution function equation of the Beta distribution.

The failure reference curves of the motor and fan are created based on international standards of motor temperature and fan vibration and these standards are described in the following section.

3.6 International Standards of Motor Temperature and Fan Vibration

International standards of the motor temperature and fan vibration are used to determine the operating endpoints of the failure reference curves. The standards are discussed as follows:

3.6.1 Motor Temperature

Motor temperature rating depends on the insulation system, and based on the insulation system, the motor is divided into different classes. The motor used for the wind tunnel belongs to F- class motor. According to the International Electrotechnical Commission (IEC) and the National

Electrical Manufacturers Association (NEMA) standard, F-class motor operating temperature ranges from -20°C to 155°C, as shown in Table 3.2 [39] and [40].

Table 3.2: F-class motor temperature ratings [39] and [40].

F-Class Motor	100 HP, 75 KW
Minimum Temperature	- 20°C
Maximum Temperature	155°C

3.6.2 Fan Vibration

The International Organization for Standardization (ISO 10816-1) provides the standard to evaluate machine vibration severity in the 600 to 12,000 RPM (10 to 200 Hz) range [41], [42]. According to the ISO 10816-1 standard, the fan used for the wind tunnel falls under the large rigid foundation (class 3) category. For vibration severity analysis, ISO 10816-1 standard uses root mean square (RMS) velocity instead of actual velocity. Table 3.3 shows the limits for different vibration stages. RMS value is used for vibration because it represents the overall magnitude of harmonic oscillation. For a set of n values (x_1, x_2, \dots, x_n), the RMS value is calculated using the Eq. (3-3)

$$x_{RMS} = \sqrt{\frac{1}{n}(x_1^2 + x_2^2 + \dots + x_n^2)} \quad (3-3)$$

For condition monitoring, whether to consider RMS velocity or actual velocity depends on the type of data acquisition device used to monitor vibration values. The reason is that there are data acquisition devices that give vibration value either in RMS velocity or in actual velocity. This research uses LabView software to create the wind tunnel condition monitoring program.

The LabView software has a RMS function. The function is used to calculate the RMS value.

Using the function actual velocity data can be converted to RMS velocity data.

Table 3.3: ISO 10816-1 standard for vibration [42].

Vibration RMS Velocity in mm/s	Class 3 Large Rigid Foundation
0 to 1.80	Good
1.81 to 7.09	Satisfactory
7.10 to 11.20	Unsatisfactory
11.21 to 45.00	Unacceptable

3.7 Assumptions Related to Failure Reference Curves

The failure reference curves are created utilizing the international standard and the information obtained from the literature review. However, a few considerations are made due to insufficient information.

- The average normal operating temperature for the motor is 45°C. The normal operating temperature is the summation of ambient temperature and temperature rise. According to the International Union of Pure and Applied Chemistry (IUPAC), 25°C is considered as the standard ambient temperature [43]. For this research, the temperature rise is chosen to be 20°C, as shown in Figure 3-6.

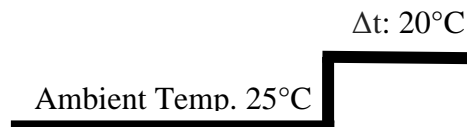


Figure 3-6: Normal operating temperature of the motor.

- The shape of the failure reference curves is concave up, as shown in Figure 3-7. The reason for choosing the concave up shape is because motor and fan performance degrades sharply at high temperature and vibration values. According to the motor instructions manual of TECO-Westinghouse Inc., the motor insulation resistance becomes approximately halved for each 10°C increase in insulation temperature above the standard maximum temperature [44]. This information implies that at high temperatures, the insulation resistance decreases sharply. As a result, the probability of motor failure increases rapidly. The vibration has similar impacts on fan failure. When vibration is low, the probability of fan failure is low, and the probability of fan failure increases remarkably when vibration value is high.

To create the curve, the probability of motor failure is considered to be 1% at the normal operating temperature, 45°C and 80% at 150°C. The reason is that the F-class motor is highly unlikely to fail because of temperature-related issues when it is running at a very low temperature, 45°C. Besides, the reason for choosing 80% probability at 150°C is because, towards the maximum temperature limit, a little change in temperature will have a greater impact on the motor's performance degradation. This performance degradation will lead to severe damage to the motor and increase the probability of motor failure.

For the fan, the probability of fan failure is considered to be 1% when vibration is 1.8 mm/s and 80% at 6.5 mm/s. The reason is that Table 3.3 shows that the vibration range for the Good class falls between 0 to 1.8 mm/s, so between this range probability of failure is low. The reason for choosing 80% at 6.5 mm/s is that at a high vibration, fan performance degradation and failure probability are extremely high.

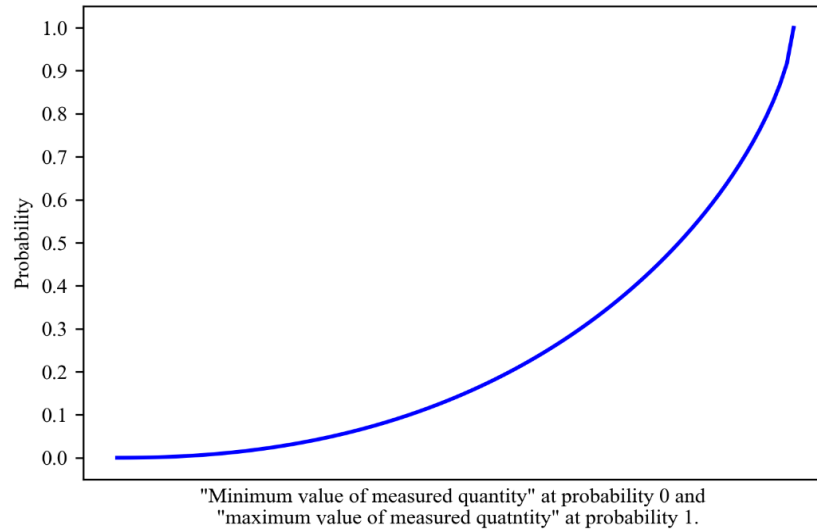


Figure 3-7: The shape of the failure reference curve is concave up.

A sensitivity analysis of these values is presented in Appendix A. The analysis shows that the impacts are low for the changes in the probability, temperature, and vibration values.

3.8 Statistical Concepts Used to Create Failure Reference Curve

The statistical concepts of cumulative distribution function (CDF) and Beta distribution are used to create the curves. The reason CDF is used because it gives accumulated probability value and the Beta distribution is used because it allows the shape of the CDF curve to be concave up.

Detailed explanations of the cumulative distribution function and Beta distribution are presented in the following sections.

3.8.1 Cumulative Distribution Function

The cumulative distribution function $F(x)$ for a continuous real-valued random variable X is defined for every number x by [45],

$$F(x) = P(X \leq x) = \int_{-\infty}^x f(t)dt \quad (3-4)$$

x represents any real number, i.e., $-\infty < x < \infty$ and $F(x)$ gives the “accumulated” probability “up to x ” [46]. $f(t)$ is the probability density function of X that satisfies the following properties [47]:

- Probability of X between two points a and b , $P(a \leq X \leq b) = \int_a^b f(t)dt$
- $f(t)$ is non-negative or $f(t) \geq 0$ for all real x .
- The total area under the graph of $f(t) = \int_{-\infty}^{\infty} f(t)dt = 1$

The cumulative distribution function, $F(x)$ satisfies the following criteria [36]:

- $F(-\infty) = 0$
- $F(\infty) = 1$
- $F(x)$ is an increasing function that means if $x < y$, the $F(x) \leq F(y)$ for all real x, y .

Figure 3-8 shows different shapes of cumulative distribution function curves.

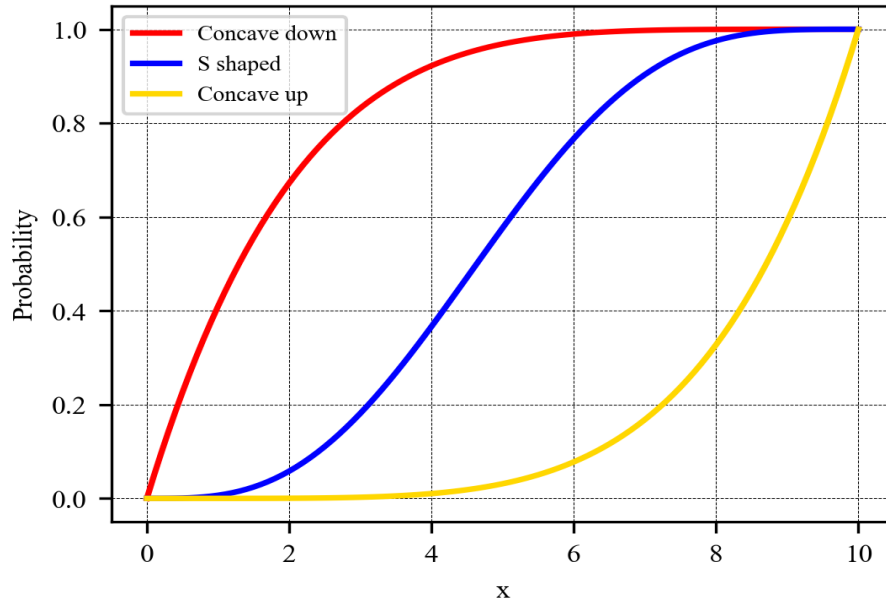


Figure 3-8: Cumulative distribution function curve.

For each x , $F(x)$ is the area under the density curve to the left of x , and $F(x)$ increases as x increases [45]. The CDF curve varies depending on the distribution. So, the research needed to find such a distribution that will allow the shape of the CDF curve to be a concave up as well as represents the physical reality of the motor and fan failure probability. For instance, when temperature and vibration values are low, a small change in values will not have much impact on failure probability; however, when the values are high, a minor change will have a significant impact on the motor and fan failure probability. After a thorough investigation, it was found that CDF of the Beta distribution can create the desired concave up shape.

3.8.2 Beta Distribution

The advantage of the Beta distribution is that it can take on different shapes [48] that will allow the shape of the failure reference curve to be concave up. Although the Weibull distribution is widely used in failure data analysis and reliability analysis [49], it is not possible to create a CDF curve concave up using Weibull distribution. So, the Beta distribution is the appropriate distribution for this research. The Beta distribution is a continuous probability distribution that has four parameters: two positive shape parameters, one scale parameter, and one location parameter [38]. The CDF of Beta distribution is defined as [50],

$$F(x) = \frac{\int_0^x (t-a)^{\alpha-1} (b-t)^{\beta-1} dt}{B(\alpha, \beta)}; \quad a \leq x \leq b; \alpha, \beta > 0 \quad (3-5)$$

where the Beta function is

$$B(\alpha, \beta) = \int_0^1 (t-a)^{\alpha-1} (b-t)^{\beta-1} dt \quad (3-6)$$

where, α and β are the shape parameters, and the variables a and b represent the location parameter and scale parameter, respectively. The shape of the CDF curve of Beta distribution is dependent on these four parameters, as shown in Figure 3-9.

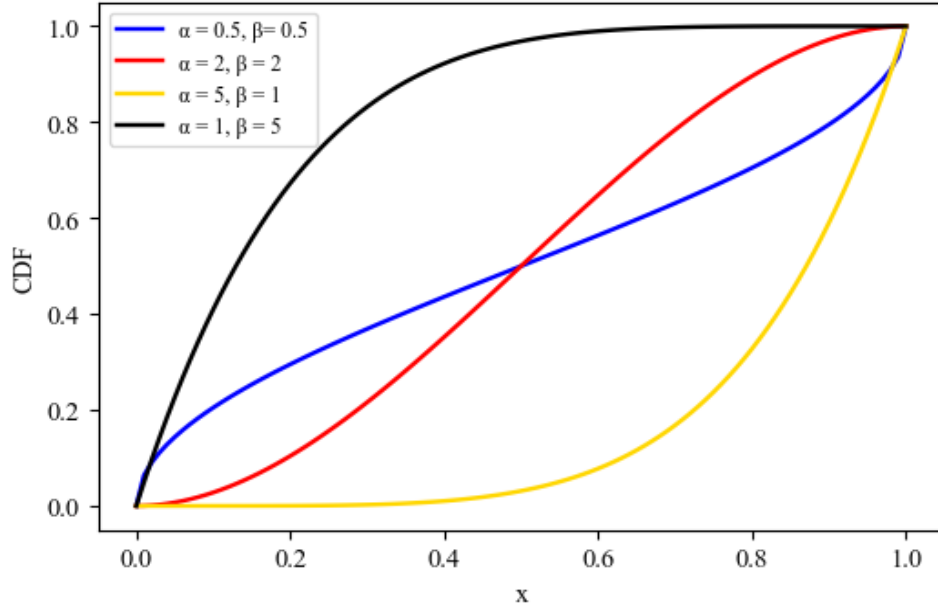


Figure 3-9: The shape of the Beta distribution CDF curve varies for different α and β values.

3.9 Determining the Parameters of the Failure Reference Curves

To create the motor and fan failure reference curves, the values of the parameters of Eq. (3-5) are needed. For this research, the location parameter, a , and the scale parameter, b values are set by the two endpoints of the failure reference curves and the values are obtained from the international standards of the motor temperature and fan vibration. To obtain the shape parameters α and β , two equations are required, and to solve two equations, two points are needed. The points are chosen in a way that the desired concave up curve passes through those points and the first point is lower than the second point on the XY-plane.

3.10 Creating the Failure Reference Curves Using CDF of the Beta Distribution

For the motor failure reference curve, the values of the location parameter, a is 25, and the scale parameter, b is 130. For the fan failure reference curve, location parameter, a is 0, and the scale parameter, b is 7.1. The two chosen points for the motor failure reference curve are (45, 0.01), and (150,0.8) and for the fan failure reference curve are (1.8, 0.01) and (6.5,0.8). The mathematical calculation is complicated to get the shape parameter values. So, programming codes are created using Python software, as shown in Appendix B. The tables in Appendix C show the values of the shape parameters, α , and β . Once all the parameter values are obtained, the failure reference curves are generated, as presented in Figure 3-10 and Figure 3-11.

The starting point of the motor failure reference curve is chosen to be 25°C. The reason is to match with the international standard of ambient temperature. As the curve starts from 25°C, so for any temperature value less than 25°C, the probability of failure will be 0. Also, Table 3.3 shows that the scale for fan vibration ranges from 0 to 45 mm/s. However, the endpoint for the fan failure curve is chosen to be 7.1 mm/s because the Unsatisfactory class for vibration starts from 7.1 mm/s. As the wind tunnel is new, so the fan vibration should not reach to the Unsatisfactory class.

It is considered that the measured variables are continuous and the variables will take on any values. As a result, if the value of the temperature or vibration changes suddenly, the proposed failure reference curve will be able to give failure probability value for the increased temperature or vibration value.

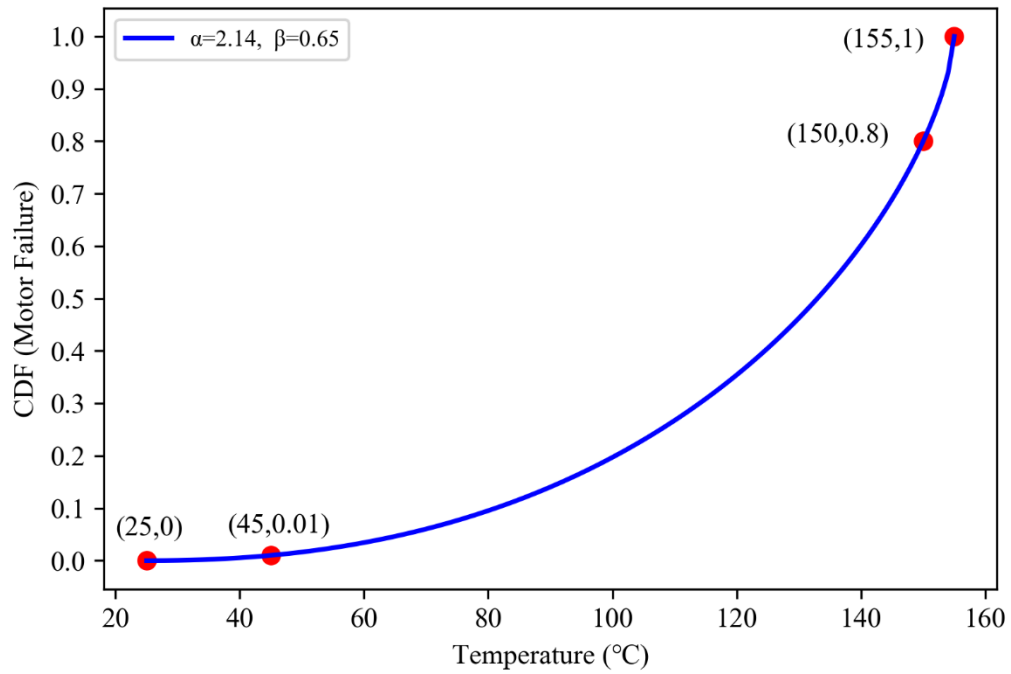


Figure 3-10: Failure reference curve for motor failure.

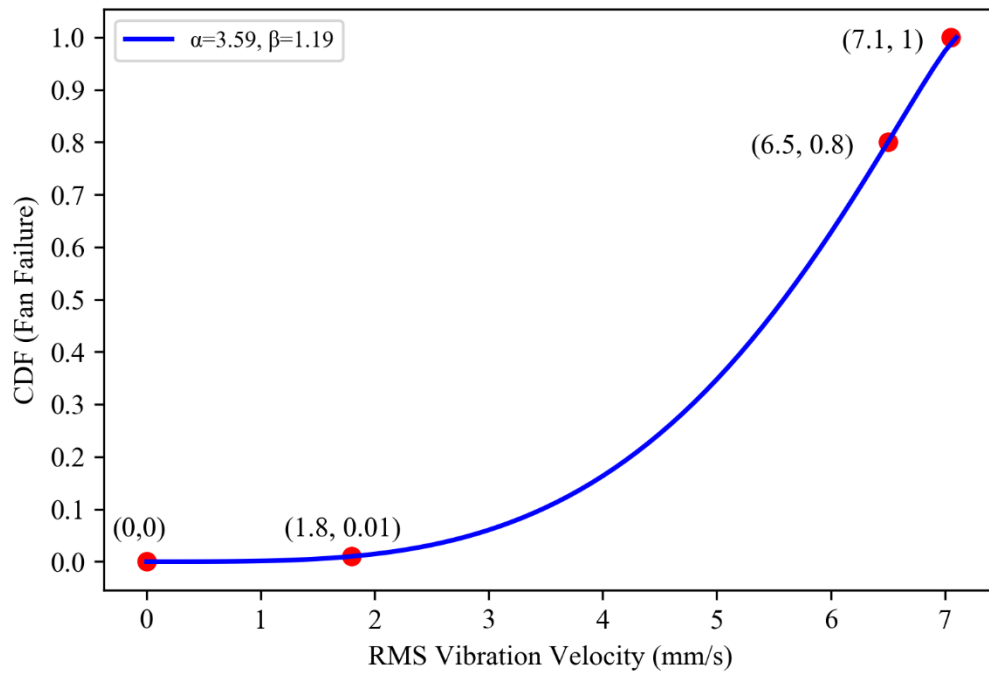


Figure 3-11: Failure reference curve for fan failure.

3.11 Classification of Motor, Fan, and System Failure

The purpose of classification is to find the normal operating range for motor temperature and fan vibration. This will also help the condition monitoring program to give feedback based on the state of the motor and fan condition. The program will change the feedback according to the temperature and vibration classes. The program will use running average and the classification will help to change the number of data points included in the running average. The probabilities of motor, fan, and system failure are classified into three classes. The idea of classifying probability is obtained from D'Ayala et al. [51]. The classes are: Normal, Moderate, and High and the probability assigned in the classes are shown in Table 3.4.

Table 3.4: Classification based on the probability of failure.

Probability of failure (%)	Classes for temperature, vibration, and system failure
$0 < \text{Probability} \leq 25$	Normal
$25 < \text{Probability} \leq 50$	Moderate
$50 < \text{Probability} \leq 100$	High

Table 3.5 shows the temperature and vibration values corresponding to the classes, and Figure 3-12 and Figure 3-13 show the temperature and vibration classes in the failure reference curves.

Table 3.5: Temperature and vibration values for each class.

Class	Temperature (°C)	Vibration (RMS velocity in mm/s)
Normal	Temperature ≤ 108	Vibration ≤ 4.5
Moderate	$108 < \text{Temperature} \leq 133$	$4.5 < \text{Vibration} \leq 5.6$
High	$133 < \text{Temperature}$	$5.6 < \text{Vibration}$

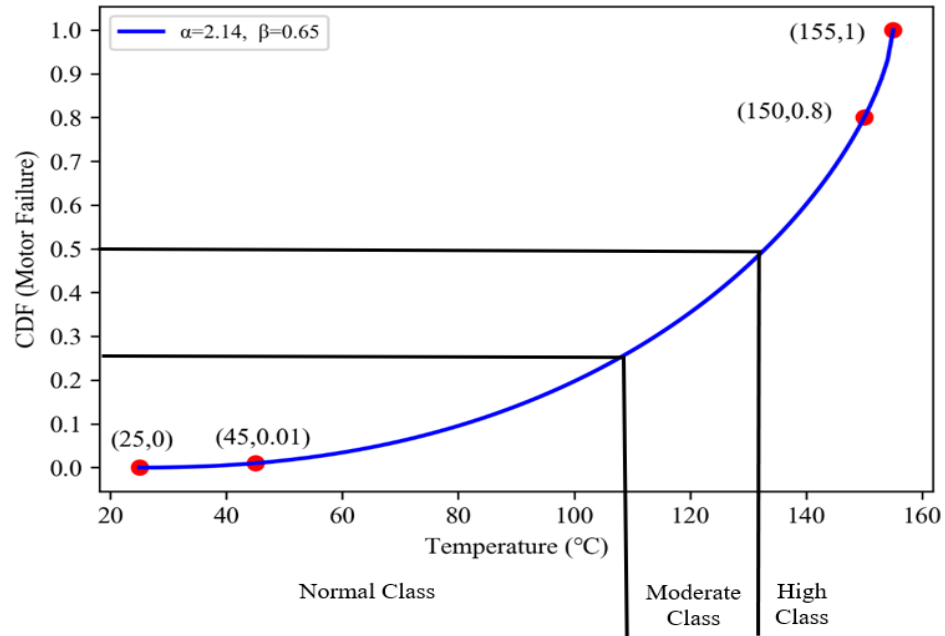


Figure 3-12: Graphical representation of the temperature classes.

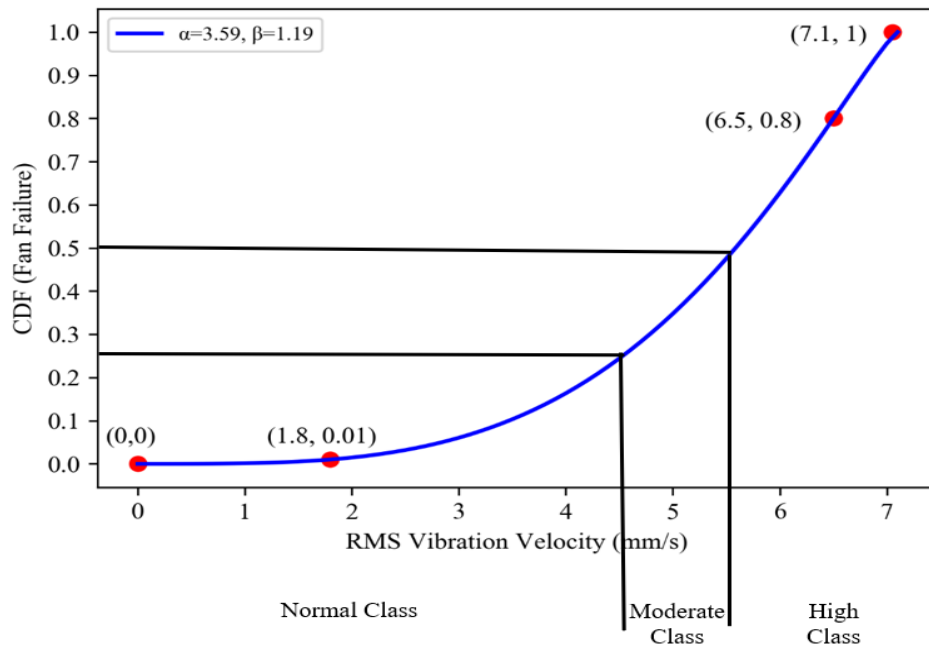


Figure 3-13: Graphical representation of the vibration classes.

3.12 Allowable Operating Range for System Failure

Even though system failure probability is classified into three classes, the system should not operate in a state when the probability of failure is high. For this reason, the condition monitoring program will not allow the system failure probability to reach the High class. So, the maximum allowable system failure probability will be up to the Moderate class or 50%.

3.13 Running Average

The condition monitoring program will use the running average to smooth spikes in the temperature and vibration signals. The running average is a concept that moves the average values. It computes the average of a set of data over a specified number of periods [52]. When new data becomes available, running average drops the old data and moves the average values along the time scale. The advantages of running average are that it is a simple way to smooth short-term fluctuations in a signal and reduces the impact of random spikes. The number of running average points affects how the running average reacts to the signal. The higher the running average points are, the lesser it is to respond to signal fluctuations. Figure 3-14 shows that the impact of fluctuations reduces as the number of running average points increases.

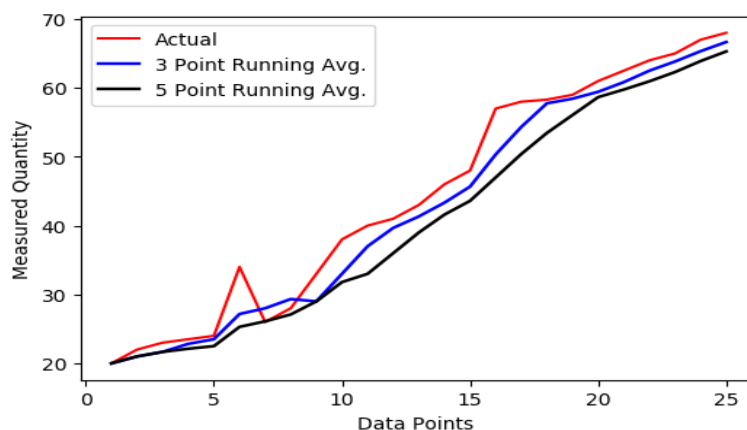


Figure 3-14: Example of running average.

4. Implementation

In this chapter, a LabView software-based condition monitoring program is presented. The program is designed to determine the wind tunnel failure probability as well as monitor motor and fan conditions. This program is capable of performing actual condition monitoring if actual sensor data are obtained using data acquisition devices. This chapter includes short descriptions of the statistical concepts that are used to create the program. The chapter also demonstrates the program functionalities using simulated data that represent the actual sensor data.

4.1 Overview of LabView

Laboratory Virtual Instrument Engineering Workbench (LabView) is a visual programming language that was primarily developed to facilitate instrumentation control and/or monitor machine/equipment test data acquisition, and data analysis [53]. LabView consists of two parts: a front panel and a block diagram. The front panel is used as the user interface and the basic elements of the front panel are classified as controls and indicators. The block diagram is where program code exists, and the code is written using blocks.

4.2 Human-Machine Interface Design

To fulfill the primary purpose of this thesis, a virtual instrument (VI) is created and the VI runs within the LabView environment. The human-machine interface is shown in Figure 4-1. The LabView program considers motor temperature and fan vibration as input signals. It displays, analyzes, and stores temperature and vibration data. Furthermore, the program provides text and visual warnings based on motor temperature and fan vibration.

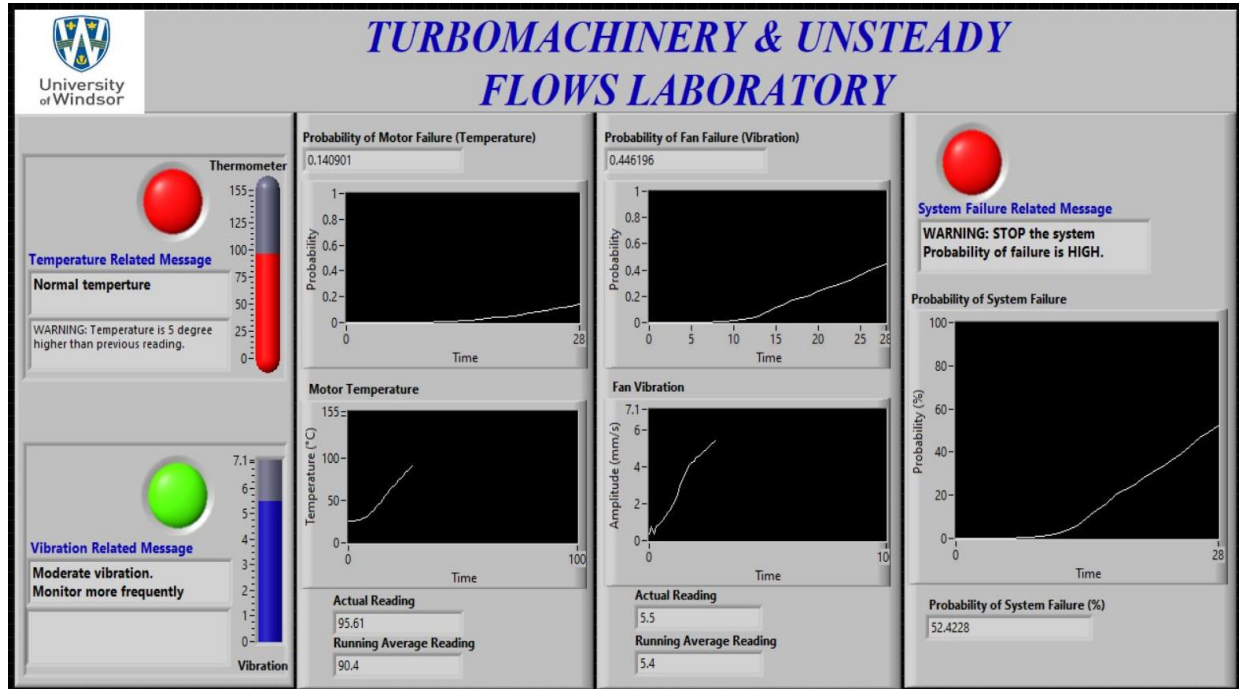


Figure 4-1: Human-machine user interface.

4.3 Statistical Concepts Used for Data Analysis

The LabView program uses statistical concepts: running average, CDF of the Beta distribution, and union rule of probability to perform condition monitoring. The description of the concepts are as follows:

4.3.1 Running Average

For the LabView program, the running average is used to smooth the effect of signal fluctuations. The criterion for choosing the appropriate number of running average data points may be related to several factors such as data sampling rate and the physical behavior of the motor temperature and fan vibration. For this research, it is considered that the effect of signal

fluctuations will be low when the values of temperature and vibration are low. For this reason, in the LabView program, the number of running average data points used for each class decreases as the probability of failure increases. Table 4.1 shows the number of data points used for each class. Using the running average concept will help to reduce misleading warning messages in the LabView user interface. For instance, if a signal is in the Moderate class and a high spike adds up to the signal, it might cause the program to display that the signal is in the High class.

Table 4.1: Number of running average points used for different classes.

	Temperature (Class)	Vibration (Class)
5 Point Running Average	Normal	Normal
3 Point Running Average	Moderate	Moderate
Actual Reading	High	High

4.3.2 CDF of the Beta Distribution

The program uses failure reference curves, as discussed in Section 3.8 to determine the probabilities of motor and fan failure. As the failure reference curves are based on CDF of the Beta distribution, the LabView program uses the Probability VIs palette because it has a Beta CDF function. The Beta CDF function requires shape parameter values to generate probability values from an input signal. The shape parameter values are obtained from the Python code as discussed in the previous chapter. Two different functions are created to process temperature and vibration signals. Once the temperature and vibration signals pass through the Beta CDF

functions, equivalent probability values are generated. These probability values are used as the variables of the probability-based model.

4.3.3 Union Rule of Probability

To get the overall probability of system failure, the LabView program uses the probability-based model as presented in Section 3.3. The model consists of two variables motor temperature and fan vibration. The values of the variables are obtained from the Beta CDF functions as explained in the preceding section.

4.4 The Framework of Program Operations

The high-level program operations are shown in Figure 4-2. At the beginning of the program, the program will read temperature and vibration data. Then the program will calculate running average according to the temperature and vibration classes and store the data into Excel files. After that, the program will display running average values through waveform charts, and at the same time, the program will show text and visual messages based on the running average values.

Next, the program will compare temperature and vibration data with the failure reference curves to obtain the probabilities of motor and fan failure and plot the probability values in the waveform charts. Then the program will calculate the probability of wind tunnel failure using the probability-based model and display the probability values using a waveform chart. The program will also give warning messages according to the probability of failure values.

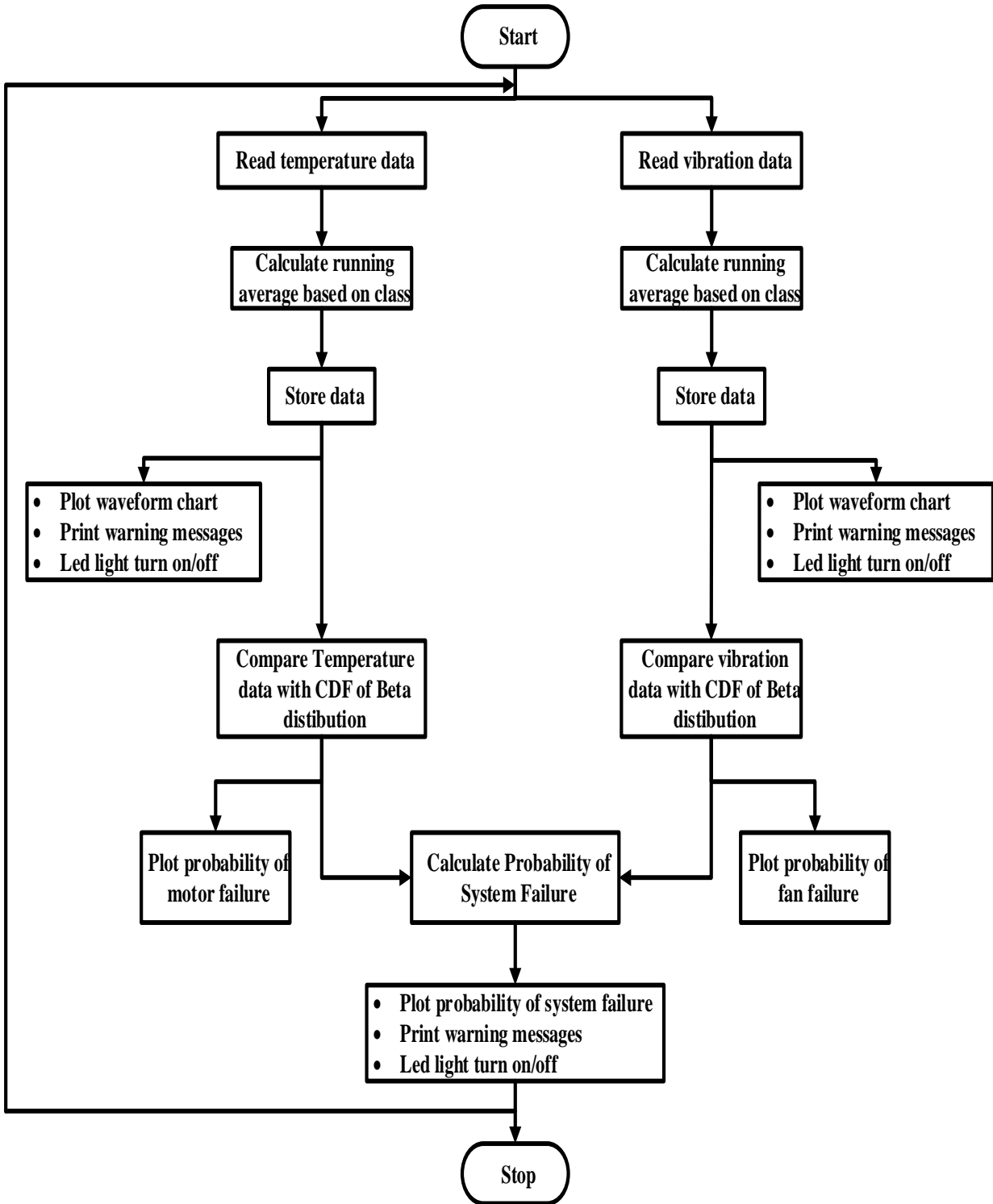


Figure 4-2: Flowchart of the LabView program.

4.5 Examples of Program Functionality Using Simulated Data

To describe the functionalities of the condition monitoring program, simulated data are used. The front panel of the LabView program is divided into eight segments, as shown in Figure 4-3.

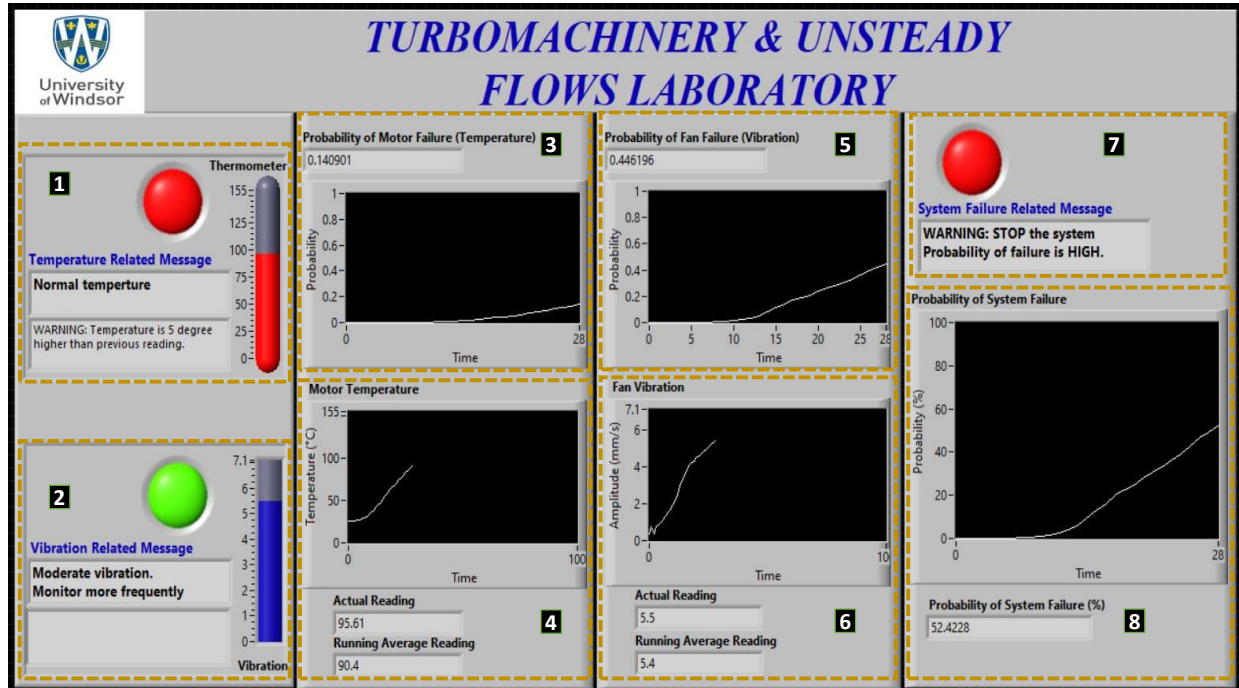
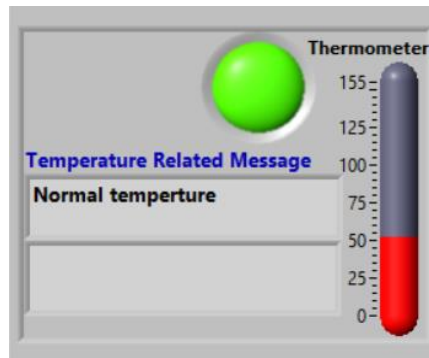


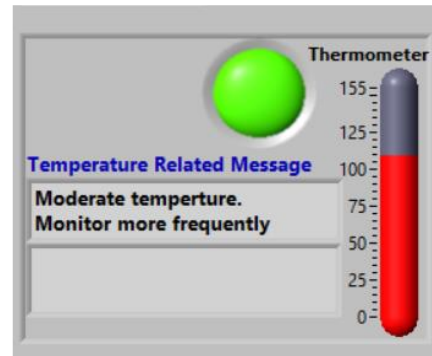
Figure 4-3: Front panel marked with segments.

4.5.1 Motor Temperature Related Messages

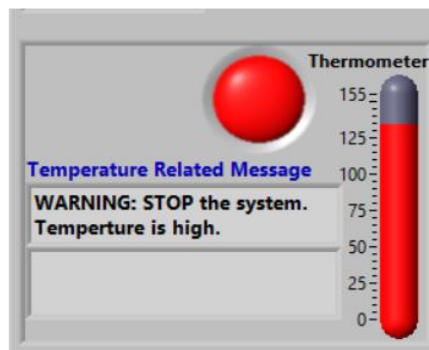
Segment 1 shows information related to the motor temperature. This segment displays text messages and turns on/off the LED light based on the temperature class, as shown in Figure 4-4. If the temperature value is in the Normal or Moderate class, the program operates normally; however, if the temperature value reaches the High class, the program turns on the LED light and displays a warning message to stop the wind tunnel. The red vertical bar on the right side shows the actual temperature readings.



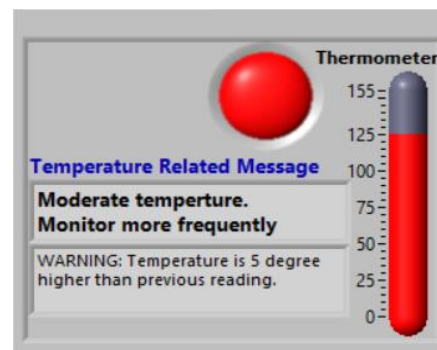
a)



b)



c)



d)

Figure 4-4: Temperature related messages. (a) Normal class, (b) Moderate class, (c) High class, and (d) When the temperature difference between actual reading and previous running average reading is higher than 5°C.

The program also gives a warning message and turns on the LED light if the temperature difference between actual reading and previous running average reading is higher than 5°C. The reason for considering 5°C is reasonable can be justified from the temperature measurement done by Karakoulidis et. al [54]. Karakoulidis et. al measured the temperature of a F-class motor's windings, core area, and ball bearing using different loads. For 80% load, the temperature was measured for 20 minutes with a sample rate of one reading per minute. The readings of the windings, core, and ball bearing show that in almost all cases, the difference between two consecutive readings is close to 5°C and does not exceed 5°C. So, choosing 5°C is reasonable because it will be alarming if the difference is higher than 5°C. Besides, to monitor

the temperature using this program, the intended sampling frequency is one reading per minute that is obtained from the measurement process of Karakoulidis et. al [54].

4.5.2 Fan Vibration Related Messages

Segment 2 displays fan vibration-related messages. The functionalities of this segment are the same as the previous segment. The program shows text messages and visual warnings corresponding to the vibration class, as shown in Figure 4-5. The blue vertical bar indicates the actual vibration readings.

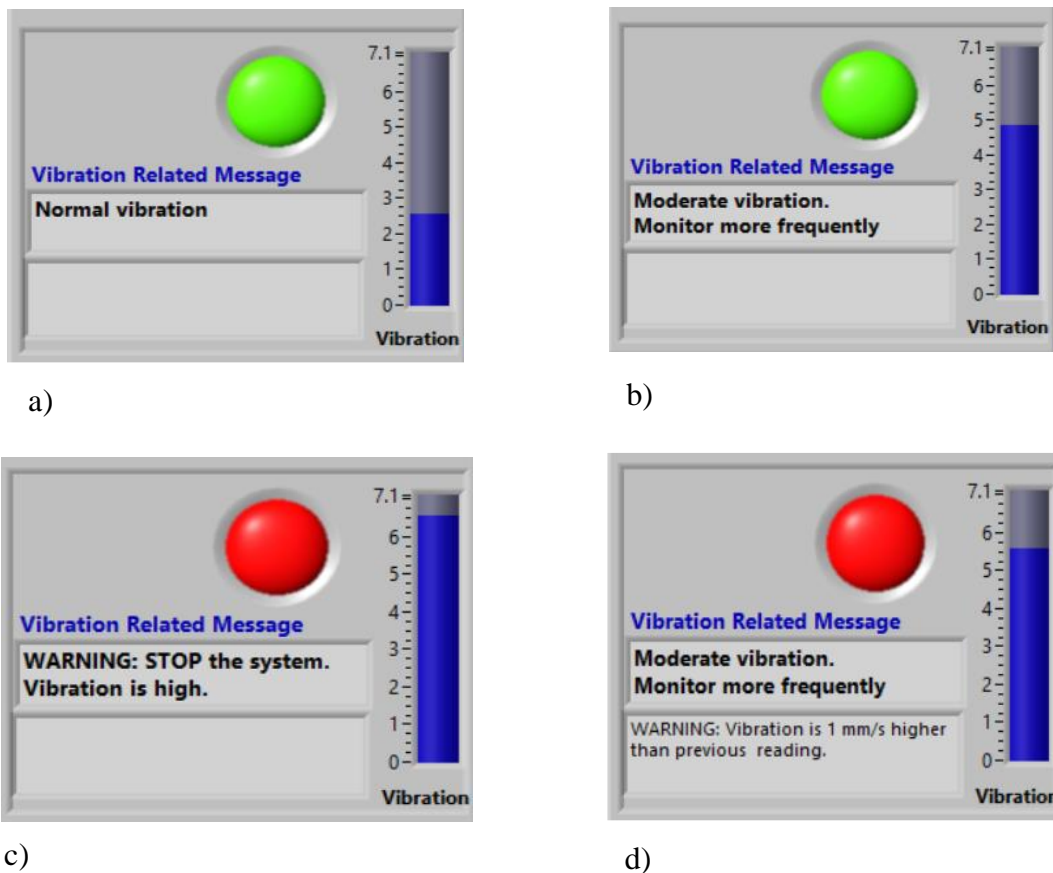
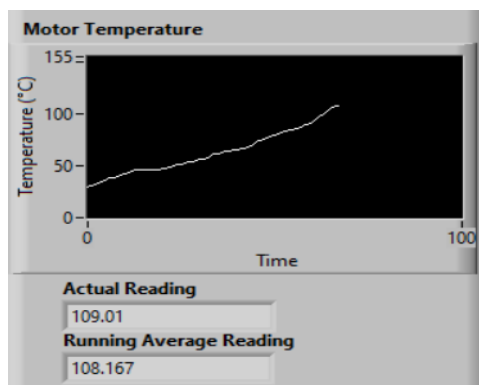


Figure 4-5: Vibration related messages. (a) Normal class, (b) Moderate class, (c) High class, and (d) When the vibration difference between actual reading and previous running average reading is higher than 1mm/s.

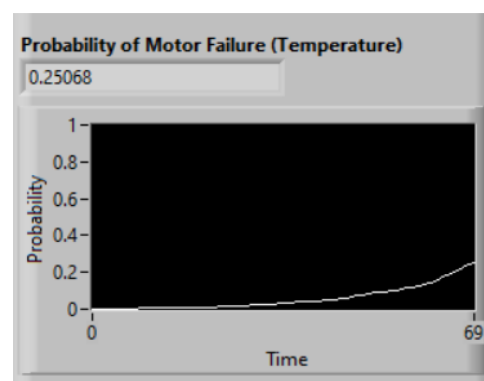
Besides, the user will see a warning message if the vibration difference between the actual reading and the previous running average reading is higher than 1mm/s. The reason for choosing 1mm/s can be justified by the vibration analysis performed by Rastegari and Bengtsson [55]. They have measured the vibration of a gas circulation fan and used RMS values in mm/s unit. Their analysis shows that at normal operating conditions, the difference between two consecutive vibration readings is less than 1mm/s. So, considering 1mm/s is reasonable to observe an abrupt increase between two consecutive vibration readings. Using the program, the intended sampling frequency for vibration is one reading per second.

4.5.3 Motor Condition Related Information

Segment 3 and 4 display motor conditions through the waveform charts and the charts show the temperature running average values and the probabilities of motor failure, as shown in Figure 4-6. In segment 3, the program uses the failure reference curve concept, as discussed in section 4.3.2. The program passes the temperature running average values through the Beta CDF function and outputs the corresponding failure probability values. Besides, the program shows the temperature running average readings and actual readings numerically in segment 4.



a)



b)

Figure 4-6: Motor condition related information. (a) Motor temperature reading, and (b) Probability of motor failure reading.

4.5.4 Fan Condition Related Information

The functionalities of segments 5 and 6 are about fan conditions. In these segments, fan vibration readings and probabilities of fan failure are shown using waveform charts and numerical data, as shown in Figure 4-7. The program passes running average values through the LabView Beta CDF function to determine the probabilities of fan failure.

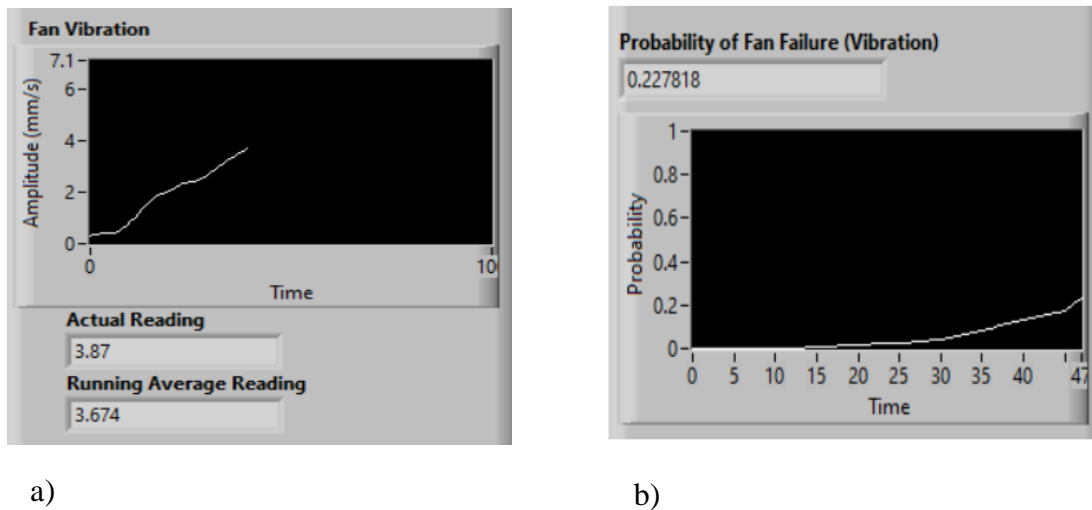
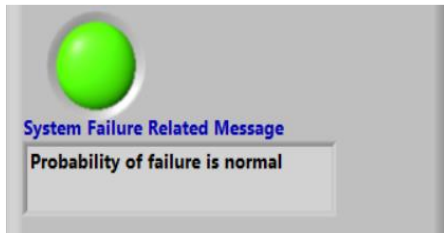


Figure 4-7: Fan vibration-related information. (a) Fan vibration reading, and (b) Probability of fan failure reading.

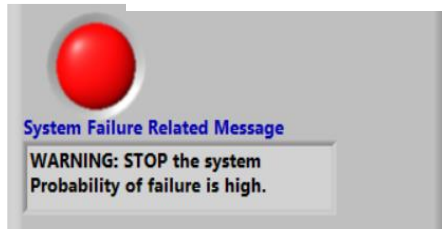
4.5.5 System Failure Related Information

System failure information is shown in segments 7 and 8. Segment 7 displays system failure related text and visual messages, and segment 8 shows the probability of system failure using waveform chart and numerical value. The probability of system failure is determined using the probability-based model. The program considers the allowable probability of system failure up to 50% probability because in Table 3.4 the Moderate class is considered up to 50%. The program displays messages based on the probability value, as shown in Figure 4-8. If the probability is

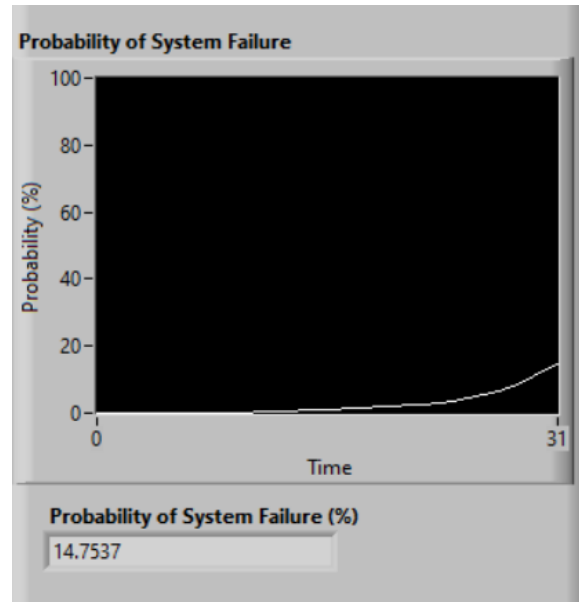
higher than 50%, the program turns on the LED light and displays a warning message to stop the wind tunnel operations.



a)



b)



c)

Figure 4-8: Information related to system failure. (a) Message for the allowable probability of failure, (b) Message for the high probability of failure, and (c) Probability of system failure.

5. Summary, Contributions, and Future Work

5.1 Summary

To create a condition monitoring program, this thesis presents a literature review that investigates the most likely causes of wind tunnel components motor, fan, and inverter failures. FTA was used to map the root causes of wind tunnel components failure. From the knowledge learned from the literature review and FTA, it was found that motor temperature and fan vibration are the most likely causes of wind tunnel failure. A statistical model was created using the union rule of probability to calculate the failure probability of the wind tunnel. The thesis presents failure reference curves to determine the variables of the model and the curves were created based on the international standards as well as the concept of CDF of the Beta distribution.

Furthermore, the thesis presents a condition monitoring program that was created using LabView software. The program helps to determine the motor and fan conditions in terms of temperature and vibration, respectively. The program was developed based on the statistical concepts running average, CDF of the Beta distribution, and addition rule of probability to analyze the temperature and vibration signals. Besides, the program gives feedback to the wind tunnel user.

There are some valuable lessons learned from the challenges of this project. Developing the condition monitoring program was challenging for several reasons. It was a difficult task to

find the appropriate parameters for the program that needs to be monitored using the program and determine the parameter values using CDF of the Beta distribution. Besides, implementing the statistical concepts in the program and having an accurate mathematical calculation to evaluate the signals were also challenging.

5.2 Thesis Contributions

The main contribution of this research is that it has developed a novel condition monitoring program. The program has a user-friendly human-machine interface, so in the future, anyone will be able to use the program without difficulty. The thesis includes a well-thought-out FTA for motor, fan, and inverter failures. The research also contributes to identify the most likely causes of the wind tunnel components failure. Furthermore, the thesis proposes failure reference curves to determine the probabilities of motor and fan failure. The curves also help to find the normal operating range for motor temperature and fan vibration.

5.3 Conclusion

Most importantly, with the help of the developed program, when students will work on the wind tunnel, they will be able to make appropriate decisions in case of abnormal temperature and vibration readings. The real-time feedback from the waveform charts, text messages, and the LED indicator light will assist the wind tunnel user to avoid failure and provide a safe operating environment at the wind tunnel lab. Furthermore, evaluating the temperature and vibration data, the user will be able to notice early warning signs of motor and fan failure.

5.4 Research Limitations

There are several limitations to this project. The limitations are listed as follows:

- This research is limited to temperature and vibration variables because these variables show the most obvious signs of motor and fan failure. This research does not consider other variables that will have a reasonable impact on motor and fan failure. For instance, aging factors: thermal aging, electrical aging, environmental aging, and mechanical aging of the components were not considered for the system failure model. Over time the aging factors may have a significant impact on motor and fan failure because these factors are affected by various circumstances such as weather conditions, voltage fluctuation, current fluctuation, temperature variation, etc. [56].
- The proposed failure reference curves are limited in several ways. First, it was found from the literature that at high temperature and vibration values, the motor and fan failure probabilities are high, so the shape of the curves were considered as concave up. Second, the normal operating temperature of the motor was chosen to be 45°C because the study did not have data acquisition devices to measure the actual temperature data. Finally, failure probability values were chosen for the motor and fan failure because those values were not found in the literature review, and the manufacturers did not share that information. Although the failure reference curves have several constraints, the sensitivity analysis in Appendix A shows the impacts of these values. The analysis shows that impacts on the motor and fan failure probability are small because of the change in values.

5.5 Future Research

There are great opportunities for future research to improve the proposed condition monitoring program. The program was tested using simulated data to verify the program functionalities. To use the program for real-world applications, future research should consider using temperature and vibration data acquisition devices that are compatible with the LabView software.

One of the objectives of this project was to give the LabView program complete authority to shut down the wind tunnel if the program detects any abnormality in temperature and vibration signals. This goal was not fulfilled due to time constraints and a lack of data acquisition devices. However, as part of the objective, a remote motor control program was developed using the LabView software. The front panel and block diagram of the program are shown in Appendix D. The program helps the user to control the motor rpm speed and rotating direction. Future research is needed to fulfill this unfinished objective.

The research only deals with temperature and vibration variables. To create a better condition monitoring program, future research should include additional variables in the LabView program. Material aging is an important factor for component failure, so for future work, it is recommended to consider the aging factors in the system failure model. The aging factors such as electrical aging and mechanical aging can be evaluated using the Fourier transform, wavelet transform, and artificial neural network [57] and [58]. Currently, the program uses a lookup table to display warning messages to the user. In the LabView program, the machine learning concept artificial neural network can be used for the decision-making of displaying warning messages [59]. The artificial neural network has three layers input layer, hidden layer, and output layer and the hidden layer is the information processing layer of the artificial neural network [60]. The artificial neural network can be trained for the normal

conditions of the temperature and vibration signals and if any abnormality happens in the signals the artificial neural network will display warning messages.

Furthermore, the program stores temperature and vibration data into excel files for future use. Evaluating those data to verify how the motor and fan performance change over time will be significant future work. Finally, predicting remaining useful life (RUL) is one of the recommended tasks in condition monitoring, so future studies are suggested to predict remaining useful life for the motor and fan.

References

- [1] N. W. Orheim, “Beamforming for condition monitoring,” M.S. thesis, Dept. of Phy., Univ. of Oslo, Oslo, Norway, 2017.
- [2] M. Karlsson and F. Hörnqvist, “Robot condition monitoring and production simulation,” Ph.D. dissertation, Dept. Civilingenjör, Maskinteknik, Luleå Tekniska Univ., Institutionen för teknikvetenskap och matematik, Luleå, Sweden, 2018.
- [3] J. Sjölander, “Non-invasive technologies for condition monitoring of synchronous motors,” Ph.D. dissertation, Uppsala Univ., Uppsala, Sweden, 2013.
- [4] L. C. Ming, “Magnetoelectric smart current sensors for wireless condition monitoring applications,” Ph.D. dissertation, Dept. Elect. Eng., The Hong Kong Polytechnic University, Hong Kong, 2011.
- [5] S. Bakhri, N. Ertugrul, W. L. Soong, and S. Al-Sarawi, “Investigation and development of a real-time on-site condition monitoring system for induction motors,” *2007 Australas. Univ. Power Eng. Conf. AUPEC*, no. August, 2007.
- [6] I. Zaman, “Condition monitoring of electric components,” M.S. thesis, Dept. Elect. Eng., Lamar Univ., Beaumont, Texas, USA, 2017.
- [7] A. Zachrison, “Fluid power applications using self-organising maps in condition monitoring,” Ph.D. dissertation, Dept. of Mgmt. and Eng., Linköping Univ. Institute of Technology, Linköping, Sweden, 2008.
- [8] C. Yang, Z. Qian, Y. Pei, and L. Wei, “A data-driven approach for condition monitoring of wind turbine pitch systems,” *Energies*, vol. 11, no. 8, 2018.
- [9] K. Ágoston, “Fault detection of the electrical motors based on vibration analysis,” *Procedia Technol.*, vol. 19, pp. 547–553, 2015.

- [10] K. A. Reay, "Efficient fault tree analysis using binary decision diagrams," Ph.D. dissertation, Loughborough Univ., Loughborough, United Kingdom, 2002.
- [11] K. D. Sharma and S. Srivastava, "Failure mode and effect analysis (FMEA) implementation: a literature review," *J. Adv. Res. Aeronaut. Sp. Sci.*, vol. 5, no. 2, pp. 2454–8669, 2018.
- [12] J. Gould, M. Glossop, and A. Ioannides, "Review of hazard identification techniques," Health and Safety Laboratory, United Kingdom, 2000. [Online]. Available: https://www.hse.gov.uk/research/hsl_pdf/2005/hsl0558.pdf.
- [13] J. Phillips and L. Simmonds, "Use of process mapping in service improvement," *Nurs. Times*, vol. 109, no. 17–18, pp. 24–26, 2013.
- [14] M. D. Sherwin, "An optimized resource allocation approach to identify and mitigate supply chain risks using fault tree analysis," Ph.D. dissertation, Dept. Ind. and Syst. Eng., Mississippi State Univ., Mississippi, USA, 2018.
- [15] R. N. Bell, D. W. McWilliams, P. O'Donnell, C. Singh, and S. J. Wells, "Report of large motor reliability survey of industrial and commercial installations, part I," *IEEE Trans. Ind. Appl.*, vol. IA-21, no. 4, pp. 853–864, 1985.
- [16] F. S. Al Badawi and M. Al Muhaini, "Reliability modeling and assessment of electric motor-driven systems in hydrocarbon industries," *IET Electr. Power Appl.*, vol. 9, no. 9, pp. 605–611, 2015.
- [17] A. H. Bonnett, "Root cause ac motor failure analysis," *IEEE Rec. Conf. Pap. - Annu. Pet. Chem. Ind. Conf.*, pp. 85–97, 1999.
- [18] R. K. Mobley, "Fans, blowers, and fluidizers," in *Maintenance Fundamentals*, Burlington, MA, USA, Elsevier, 2004, ch. 15, pp. 299-316.

- [19] X. Tian, "Cooling fan reliability: failure criteria, accelerated life testing, modeling and qualification," *IEEE Annu. Reliab. Maintainab. Symp.*, 2006.
- [20] "Fiberglass centrifugal fan installation, operation and maintenance manual," Greenheck, Schofield, Wisconsin, United States. Accessed: Mar. 23, 2020. [Online]. Available: https://content.greenheck.com/public/DAMProd/Original/10001/474051BCSW-FRP_iom.pdf.
- [21] A. Golnas, "Pv system reliability: an operator's perspective," *IEEE Photovolt. Spec. Conf.*, no. Part 2, pp. 1–6, doi: 10.1109/pvsc-vol2.2013.6656744, 2012.
- [22] "A510 Inverter," TECO-Westinghouse Inc., Cambridge, ON, Canada, Accessed: Mar. 23, 2020. [Online]. Available: https://www.tecowestinghouse.ca/wp-content/uploads/A510_instruction_manual.pdf.
- [23] S. Baschel, E. Koubli, J. Roy, and R. Gottschalg, "Impact of component reliability on large scale photovoltaic systems' performance," *Energies*, 2018, vol. 11, no. 6, p. doi: 10.3390/en11061579.
- [24] G. T. Klise, O. Lavrova, and R. Gooding, "PV system component fault and failure compilation and analysis," Sandia National Laboratories, Albuquerque, New Mexico, USA, SAND2018-1743.
- [25] J. K. Avor and C.-K. Chang, "Reliability analysis of application of variable frequency drive on condensate pump in nuclear power plant," *J. Int. Counc. Electr. Eng.* 2019, vol. 9, no. 1, pp. 8–14, doi: 10.1080/22348972.2018.1564548.
- [26] E. Batzelis, K. Samaras, G. Vokas, and S. Papathanassiou, "Off-grid inverter faults: diagnosis, symptoms and cause of failure," *Mater. Sci. Forum*, 2016, vol. 856, pp. 315–321, doi: 10.4028/www.scientific.net/MSF.856.3.

- [27] J. V Stone, “An introduction to Bayes’ rule,” in *Bayes’ Rule: A Tutorial Introduction to Bayesian Analysis*, Sheffield, England, 3rd Ed., 2014, ch. 1, pp. 1-27.
- [28] Z. Ghahramani, “An introduction to hidden Markov models and Bayesian networks,” *Pattern Recognit. Artif. Intell.*, vol. 15, no. 1, pp. 9–42, 2001.
- [29] R. Adhikari K. and A. R.K., “An introductory study on time series modeling and forecasting,” M.S. thesis, Dept. Compt. Science, Cornell Univ., Ithaca, NY, USA, 2013.
- [30] F. E. Suter, “An approach to condition monitoring and fault diagnosis of induction machines using key performance indicators,” M.S. thesis, Dept. Elect. Eng., The Univ. of North Carolina at Charlotte, Charlotte, NC, USA, 2017.
- [31] I. Ahmed, “Investigation of single and multiple faults under varying load conditions using multiple sensor types to improve condition monitoring of induction machines,” Ph.D. dissertation, The Univ. of Adelaide, Adelaide, Australia, 2007.
- [32] N. Mehala, “Condition monitoring and fault diagnosis of induction motor using motor current signature analysis,” Ph.D. dissertation, Dept. Elect. Eng., National Institute of Technology, Kurukshetra, India, 2010.
- [33] A. Hipni, J. Sabar, H. P. Sitanggang, and H. H. Purba, “Damage analysis of centrifugal exhaust fan in air arrangement in room painting,” *Int. J. Res. Eng. Sci. Manag.* 2019, vol. 1, no. 1.
- [34] “Centrifugal fan,” Kice Industries Inc., Park City, KS USA, Accessed: Mar. 25, 2020. [Online]. Available: <http://www.kice.com/pdfs/Fan%20Manual.pdf>.
- [35] T. Raykov and G. A. Marcoulides, “Probability,” in *Basic Statistics : An Introduction with R*, Lanham, MD, USA, Rowman & Littlefield Publishers, Inc., 2013, ch. 4, pp. 43-54.
- [36] M. J. Evans, “Random variables and distributions,” *Probability and Statistics: The Science*

- of Uncertainty, Univ. of Toronto, ON, Canada.
- [37] L. R. Shenton, "Parameter estimation for the Beta distribution," *J. Stat. Comput. Simul.*, vol. 43, no. 3–4, pp. 217–228, 1992.
 - [38] A. Mahanta, "Beta Distributions," Kaliabor College, Assam, India, Mar. 25, 2020.
[Online]. Available:
https://www.kaliaborcollege.org/pdf/Mathematical_Excursion_to_Beta_Distribution.pdf.
 - [39] S. Ohta, "Temperature classes of electrical insulators," *Three Bond Tech. News*, vol. 13, no. 1, pp. 1–10, 1985.
 - [40] M. Rosu *et al.*, "Multiphysics Simulation by Design for Electrical Machines, Power Electronics and Drives," *Multiphysics Simul. by Des. Electr. Mach. power Electron. drives*, 2017, pp. 1–290, doi:10.1002/9781119103462.
 - [41] K. Listewnik, G. Grzeczka, M. Kłaczyński, and W. Cioch, "An on-line diagnostics application for evaluation of machine vibration based on standard iso 10816-1," *J. Vibroengineering*, vol. 17, no. 8, pp. 4248–4258, 2015.
 - [42] J. Robichaud and P. Eng, "Reference standards for vibration monitoring and analysis," *Bretech Eng. Ltd*, pp. 1–10, 2009.
 - [43] International Union of Pure and Applied Chemistry and Compendium, "Compendium of chemical terminology," Research Triangle Park, NC, USA, 2014.
 - [44] "Instructions For Three Phase Induction Motors," TECO-Westinghouse Inc., Cambridge, ON, Canada, Accessed: Mar. 25, 2020. [Online]. Available:
https://www.tecowestinghouse.ca/wp-content/uploads/TWMI_Manual-_Large_Cast_Iron_Frames_440_and_Larger.pdf.
 - [45] J. L. Devore, "Continuous random variables and probability distributions," in *Probability*

- and statistics for engineering and the sciences, 8th ed. Boston, MA, USA: Brooks/Cole, 2010, ch. 4, pp. 137-192.
- [46] “The cumulative distribution function for a random variable X,” [www.math.wustl.edu, http://www.math.wustl.edu/~freiwald/Math132/cdf.pdf](http://www.math.wustl.edu/~freiwald/Math132/cdf.pdf) (accessed Mar. 25, 2020).
- [47] A. Holmes, B. Illowsky, and S. Dean, “Probability density function,” *Introductory Business Statistics*, Univ. of Oklahoma, Norman, OK, USA.
- [48] K. Bury, “Beta distributions,” *Stat. Distrib. Eng.*, vol. 1, pp. 238–266, 2012.
- [49] E. Arrospide, I. Bikandi, I. García, G. Durana, G. Aldabaldetrekú, and J. Zubia, “Mechanical properties of polymer-optical fibres,” in *Polymer Optical Fibres*, Duxford, United Kingdom, Woodhead, 2017, ch. 7, pp. 201-214, 2017.
- [50] C. Walck, “Hand-book on statistical distributions for experimentalists,” University of Stockholm, Stockholm, Sweden, Sep. 2007.
- [51] D. D’Ayala *et al.*, “Assessment of the multi-hazard vulnerability of priority cultural heritage structures in the Philippines,” *ICONHIC 1st Int. Conf. Nat. Hazards Infrastruct.*, no. June, 2016.
- [52] X. F. Hui and Y. J. Wu, “Research on simple moving average trading system based on SVM,” *Int. Conf. Manag. Sci. Eng. - Annu. Conf. Proc.*, no. 71031003, pp. 1393–1397, 2012.
- [53] J. Travis and J. Kring, “The LabVIEW environment,” in *Labview for Everyone Graphical Programming Made Even Easier*, 3rd ed. New Jersey, USA, Prentice-Hall, 2006, ch. 3, pp. 125-158.
- [54] K. Karakoulidis, J. G. Fantidis, C. Potolias, P. Kogias, and D. V. Bandekas, “The temperature measurement of a single phase induction motor under different conditions,”

- ARPJ. Eng. Appl. Sci.*, vol. 11, no. 19, pp. 11495–11502, 2016.
- [55] A. Rastegari and M. Bengtsson, “A Data-Driven Approach for Condition Monitoring of Wind Turbine Pitch Systems,” *Int. Conf. Progn. Heal. Manag. PHM*.
- [56] T. L. Koltunowicz, “Accelerated insulation aging due to thermal and electrical stresses in future power grids,” M.S. thesis, Dept. of Elect. Eng., The Univ. of Nottingham, United Kingdom, 2014.
- [57] A. S. Sait, “Real-time condition monitoring and fault diagnosis of gear train systems using instantaneous angular speed (IAS) analysis,” Ph.D. dissertation, Dept. of Mech. Eng., Florida Institute of Technology, Melbourne, FL, USA, 2007.
- [58] X. Wen, “A hybrid intelligent technique for induction motor condition monitoring,” Ph.D. dissertation, Institute of Industrial Research, Univ. of Portsmouth, Portsmouth, UK, 2011.
- [59] T. Anagnostou, M. Remzi, M. Lykourinas, and B. Djavan, “Artificial neural networks for decision-making in urologic oncology,” *Eur. Urol.*, vol. 43, no. 6, pp. 596–603, 2003.
- [60] D. Delen and R. Sharda, “Artificial neural networks in decision support systems,” Dept. of Manage. Sci. and Info. Syst., Oklahoma State Univ., Stillwater, OK, USA, 2008.

Appendix A

Sensitivity Analysis of the Failure Reference Curves

The purpose of this sensitivity analysis is to show how the failure reference curves and the temperature and vibration classes change if the assumed values were different. For temperature the failure reference curve was created considering the probability of motor failure is 1% at 45°C and 80% at 150°C. Out of the four assumed values, the sensitivity analysis is performed keeping three values unchanged and using three different values for the other assumed value. Among the three values, one value is the original value that is used to create the failure reference curve and the other two values are chosen in a way that one is above the original value and another one is below the original value. The reason considering three values are adequate to perform sensitivity analysis is because it gives an overall idea about the sensitivity of the change in temperature for increasing and decreasing values. The sensitivity analysis includes figures where motor failure is considered 0.5% or 1% or 1.5% at 45°C; 1% at 40°C or 45°C or 50°C; 75%, 80% and 85% at 150°C; and 80% at 147.5°C, 150°C and 152.5°C. These are the chosen assessment criteria for this sensitivity analysis. The analysis shows that the changes in temperature class boundaries are relatively low for the changes in the values.

The failure reference curve for fan failure was obtained assuming the probability of fan failure is 1% at 1.8 mm/s and 80% at 6.5 mm/s. The sensitivity analysis includes figures where fan failure is considered 0.5% or 1% or 1.5% at 1.8 mm/s; 1% at 1.6 mm/s, 1.8 mm/s and 2 mm/s; 75%, 80% and 85% at 6.5 mm/s; and 80% at 6.3 mm/s, 6.5 mm/s and 6.7 mm/s. From the analysis, the changes in class boundaries were calculated and no significant amount of change is noticed in the vibration classes.

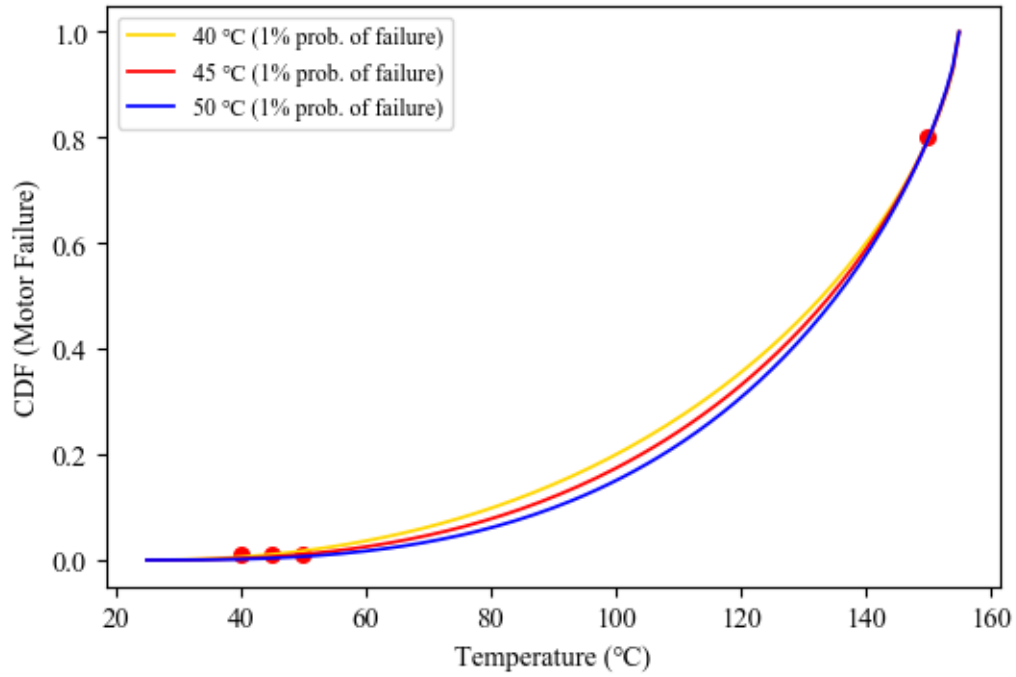


Figure A-1: Probability is 1% at 40°C or 45°C or 50°C and 80% at 150°C.

Table A.1: Temperature classes when probability is 1% at 40°C or 45°C or 50°C.

Class	Probability of failure is 1% at 40°C or 45°C or 50°C		
	40°C	45°C	50°C
Normal	Temperature ≤ 104	Temperature ≤ 108	Temperature ≤ 112
Moderate	$104 < \text{Temperature} \leq 132$	$108 < \text{Temperature} \leq 133$	$114 < \text{Temperature} \leq 135$
High	$132 < \text{Temperature}$	$133 < \text{Temperature}$	$135 < \text{Temperature}$
The temperature unit is °C.			

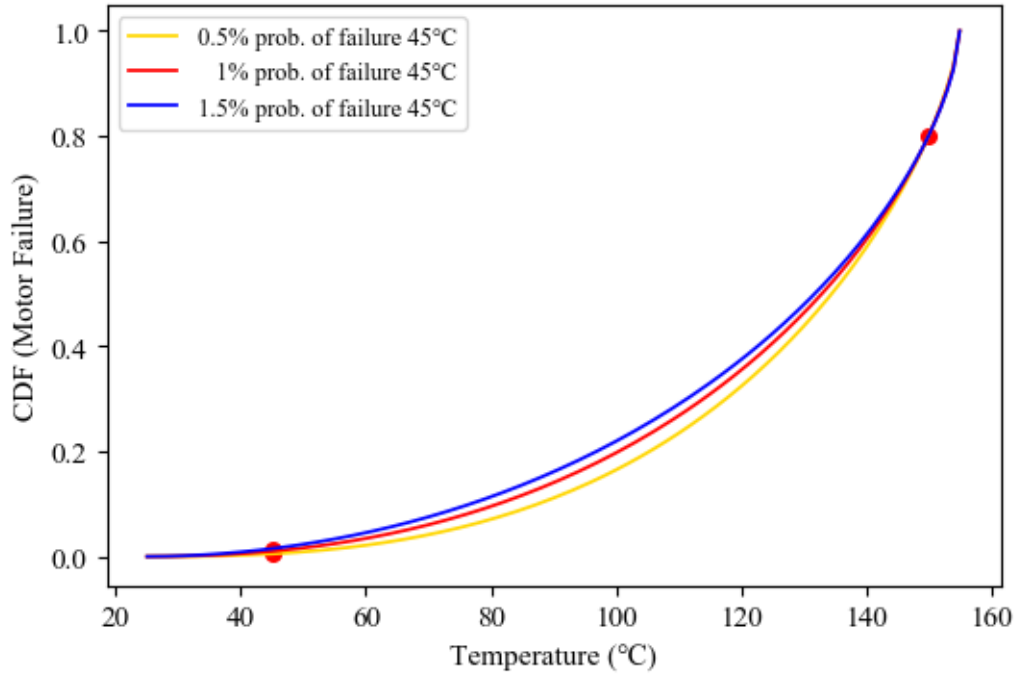


Figure A-2: Probability is 0.5% or 1% or 1.5% at 45°C and 80% at 150°C.

Table A.2: Temperature classes when probability is 0.5% or 1% or 1.5% at 45°C.

Class	Probability of failure is 0.5% or 1% or 1.5% at 45°C		
	0.5%	1%	1.5%
Normal	Temperature ≤ 111	Temperature ≤ 108	Temperature ≤ 105
Moderate	$111 < \text{Temperature} \leq 135$	$108 < \text{Temperature} \leq 133$	$105 < \text{Temperature} \leq 132$
High	$135 < \text{Temperature}$	$133 < \text{Temperature}$	$132 < \text{Temperature}$
The temperature unit is °C.			

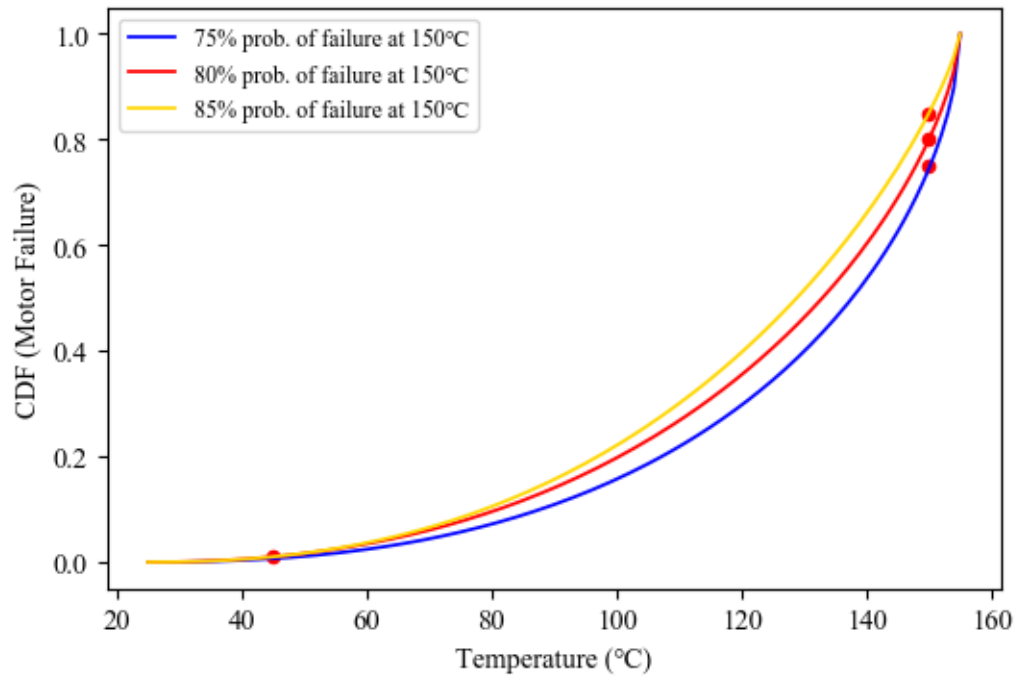


Figure A-3: Probability is 1% at 45°C and 75% or 80% or 85% at 150°C.

Table A.3: Temperature classes when prob. is 75% or 80% or 85% at 150°C.

Class	Probability of failure is 75% or 80% or 85% at 150°C		
	75%	80%	85%
Normal	Temperature ≤ 114	Temperature ≤ 108	Temperature ≤ 104
Moderate	$114 < \text{Temperature} \leq 138$	$108 < \text{Temperature} \leq 133$	$104 < \text{Temperature} \leq 129$
High	$138 < \text{Temperature}$	$133 < \text{Temperature}$	$129 < \text{Temperature}$
The temperature unit is °C.			

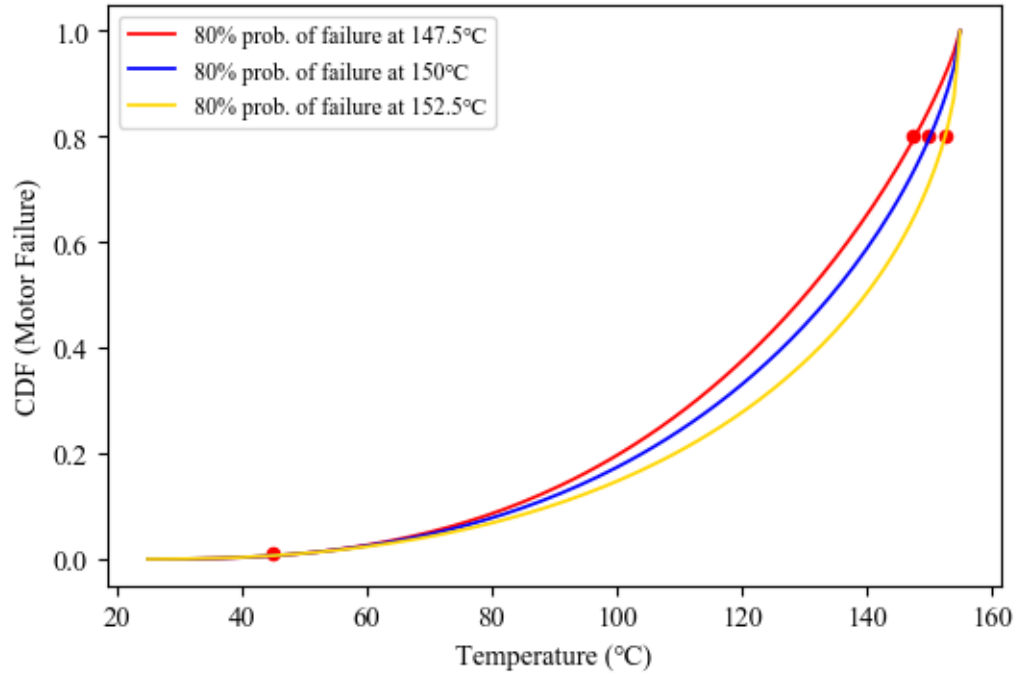


Figure A-4: Probability is 1% at 45°C and 80% at 147.5°C or 150°C or 152.5°C.

Table A.4: Temperature classes when prob. is 80% at 147.5°C or 150°C or 152.5°C.

Class	Probability of failure is 80% at 147.5°C or 150°C or 152.5°C		
	147.5°C	150°C	152.5°C
Normal	Temperature ≤ 104	Temperature ≤ 108	Temperature ≤ 114
Moderate	$104 < \text{Temperature} \leq 129$	$108 < \text{Temperature} \leq 133$	$114 < \text{Temperature} \leq 139$
High	$129 < \text{Temperature}$	$133 < \text{Temperature}$	$139 < \text{Temperature}$
The temperature unit is °C.			

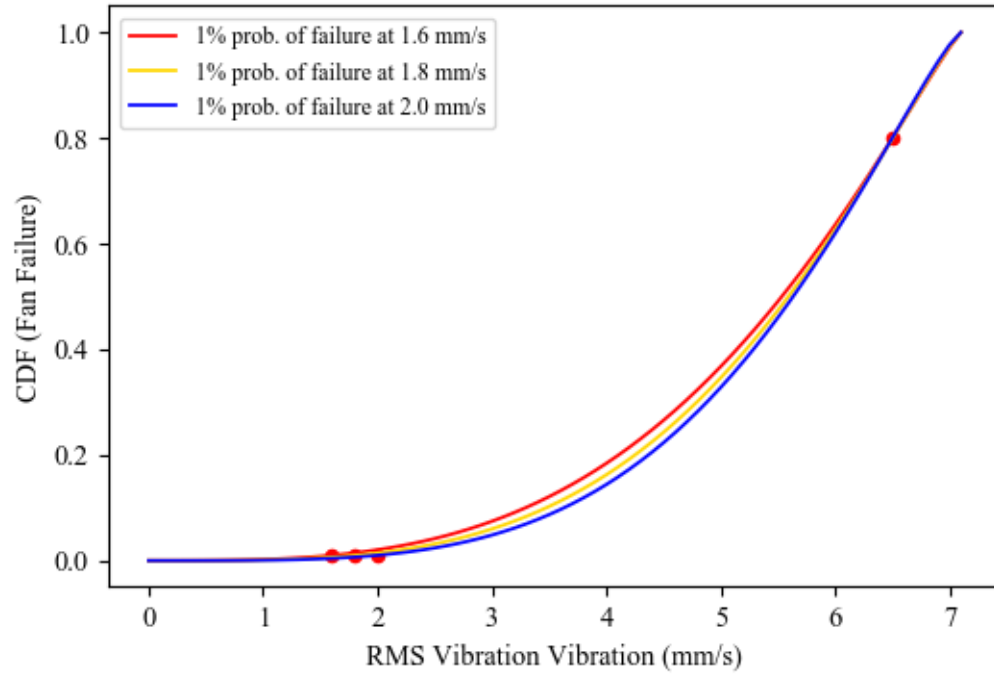


Figure A-5: Prob. is 1% at 1.6 mm/s, 1.8 mm/s, and 2 mm/s and 80% at 6.5 mm/s

Table A.5: Vibration classes when prob. is 1% at 1.6 mm/s, 1.8 mm/s, and 2 mm/s.

Class	Probability of failure is 1% at 1.6 mm/s, 1.8 mm/s, and 2 mm/s		
	1.6 mm/s	1.8 mm/s	2 mm/s
Normal	Vibration ≤ 4.4	Vibration ≤ 4.5	Vibration ≤ 4.6
Moderate	$4.4 < \text{Vibration} \leq 5.5$	$4.5 < \text{Vibration} \leq 5.6$	$4.6 < \text{Vibration} \leq 5.6$
High	$5.5 < \text{Vibration}$	$5.6 < \text{Vibration}$	$5.6 < \text{Vibration}$
The vibration unit is mm/s.			

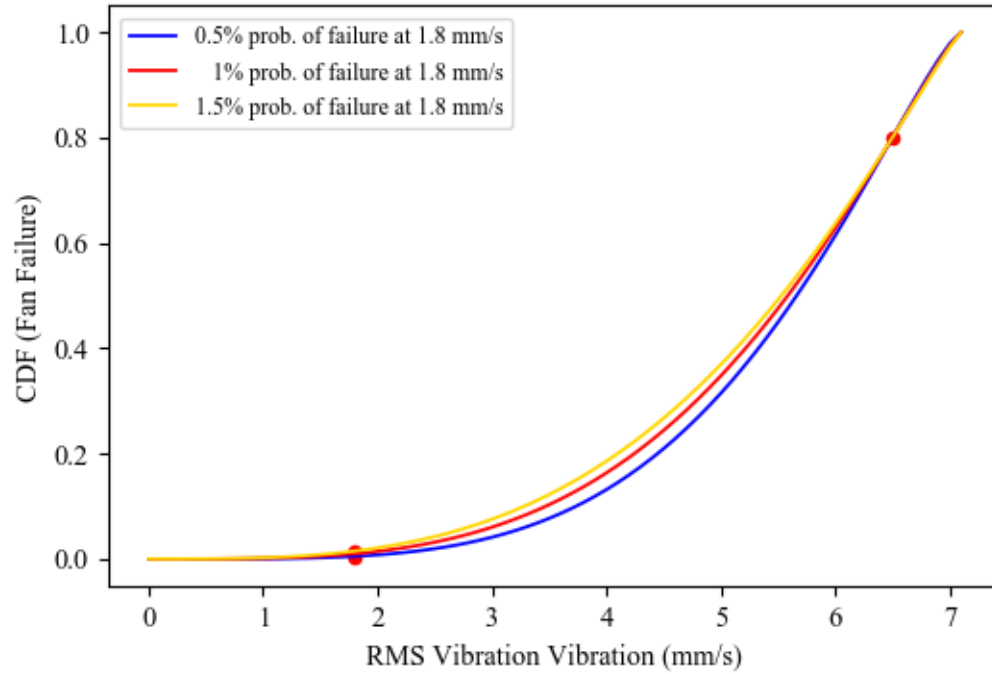


Figure A-6: Prob. is 0.5% or 1% or 1.5% at 1.8 mm/s and 80% at 6.5 mm/s.

Table A.6: Vibration classes when prob. is 0.5% or 1% or 1.5% at 1.8 mm/s.

Class	Probability of failure is 0.5% or 1% or 1.5% at 1.8 mm/s		
	0.5%	1%	1.5%
Normal	Vibration ≤ 4.7	Vibration ≤ 4.5	Vibration ≤ 4.4
Moderate	$4.7 < \text{Vibration} \leq 5.7$	$4.5 < \text{Vibration} \leq 5.6$	$4.4 < \text{Vibration} \leq 5.5$
High	$5.7 < \text{Vibration}$	$5.6 < \text{Vibration}$	$5.5 < \text{Vibration}$
The vibration unit is mm/s.			

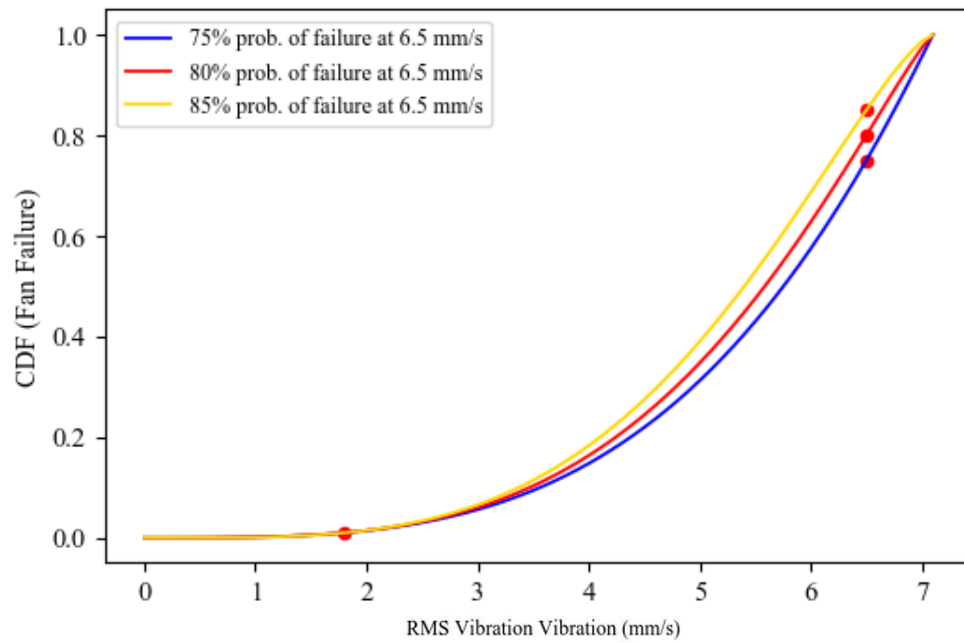


Figure A-7: Prob. is 1% at 1.8 mm/s and 75% or 80% or 85% at 6.5 mm/s.

Table A.7: Vibration classes when prob. is 75% or 80% or 85% at 6.5 mm/s.

Class	Probability of failure is 75% or 80% or 85% at 6.5 mm/s		
	75%	80%	85%
Normal	Vibration ≤ 4.7	Vibration ≤ 4.5	Vibration ≤ 4.4
Moderate	$4.7 < \text{Vibration} \leq 5.8$	$4.5 < \text{Vibration} \leq 5.6$	$4.4 < \text{Vibration} \leq 5.4$
High	$5.8 < \text{Vibration}$	$5.6 < \text{Vibration}$	$5.4 < \text{Vibration}$
The vibration unit is mm/s.			

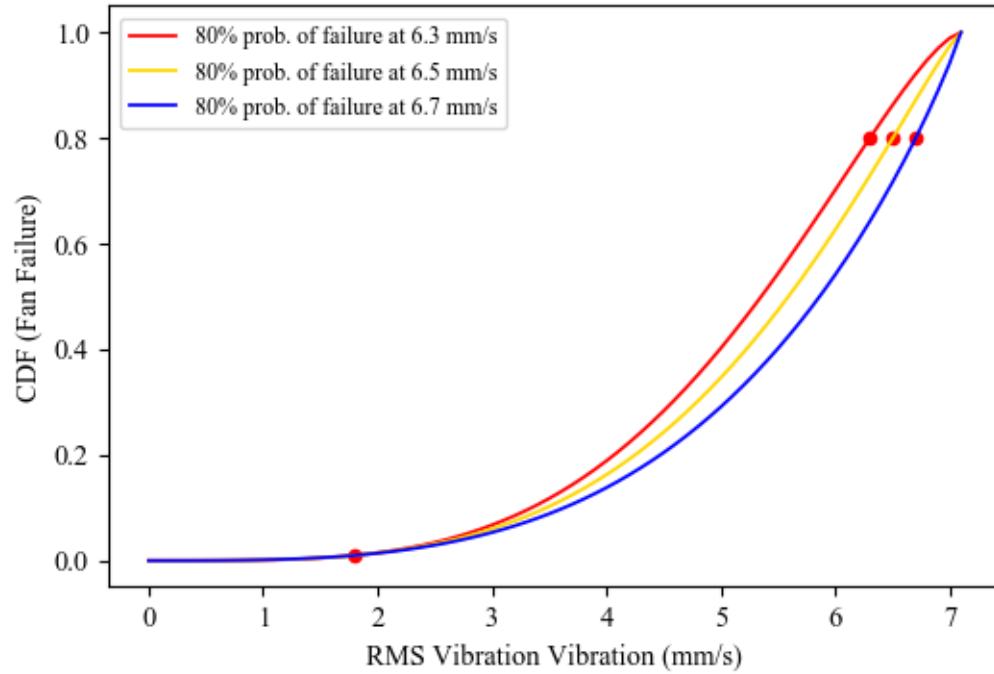


Figure A-8: Prob. is 1% at 1.8 mm/s and 80% at 6.3 mm/s, 6.5 mm/s and 6.7 mm/s.

Table A.8: Vibration classes when prob. is 80% at 6.3 mm/s, 6.5 mm/s and 6.7 mm/s.

Class	Probability of failure is 80% at 6.3 mm/s, 6.5 mm/s and 6.7 mm/s		
	6.3 mm/s	6.5 mm/s	6.7 mm/s
Normal	Vibration ≤ 4.3	Vibration ≤ 4.4	Vibration ≤ 4.8
Moderate	$4.3 < \text{Vibration} \leq 5.3$	$4.4 < \text{Vibration} \leq 5.5$	$4.8 < \text{Vibration} \leq 5.8$
High	$5.3 < \text{Vibration}$	$5.5 < \text{Vibration}$	$5.8 < \text{Vibration}$
The vibration unit is mm/s.			

Appendix B

Determining Shape Parameters (α , β) of CDF of Beta Distribution

Temperature:

```
from scipy.stats import beta
from scipy.optimize import minimize
# Loss function using Mean Squared Error
def lossfunction(x):
    alpha_shape = x[0]
    beta_shape = x[1]
    d_1 = (beta.cdf(45, alpha_shape, beta_shape, scale=130, loc=25) - 0.01)**2
    d_2 = (beta.cdf(150, alpha_shape, beta_shape, scale=130, loc=25) - 0.8)**2
    d = d_1 + d_2
    mean_squared_error = d/2
    #print ("Loss function values: ", mean_squared_error)
    return mean_squared_error
# Optimization Algorithm
print ("Nelder-Mead: ", minimize(lossfunction, x0=[0.5, 0.5], method='nelder-mead'))
#print ("TNC: ", minimize(lossfunction, x0=[0.5, 0.5], method='TNC'))
#print ("BFGS: ", minimize(lossfunction, x0=[0.5, 0.5], method='BFGS'))
#print ("CG: ", minimize(lossfunction, x0=[0.5, 0.5], method='CG'))
#print ("Powell: ", minimize(lossfunction, x0=[0.5, 0.5], method='Powell'))
```

Vibration:

```
from scipy.stats import beta
from scipy.optimize import minimize
# Create loss function using Mean Squared Error
def lossfunction(x):
    alpha_shape = x[0]
    beta_shape = x[1]
    d_1 = (beta.cdf(1.8, alpha_shape, beta_shape, scale=7.1, loc=0) - 0.01)**2
    d_2 = (beta.cdf(6.5, alpha_shape, beta_shape, scale=7.1, loc=0) - 0.8)**2
    d = d_1 + d_2
    mean_squared_error = d/2
    #print ("Loss function values: ", mean_squared_error)
    return mean_squared_error
# Optimization Algorithm
print ("Nelder-Mead: ", minimize(lossfunction, x0=[0.5, 0.5], method='nelder-mead'))
#print ("TNC: ", minimize(lossfunction, x0=[0.5, 0.5], method='TNC'))
#print ("BFGS: ", minimize(lossfunction, x0=[0.5, 0.5], method='BFGS'))
#print ("CG: ", minimize(lossfunction, x0=[0.5, 0.5], method='CG'))
#print ("Powell: ", minimize(lossfunction, x0=[0.5, 0.5], method='Powell'))
```

Plotting failure reference curve for temperature:

```
from scipy.stats import beta
import matplotlib.pyplot as plt
import numpy as np
fig= plt.figure(figsize=(6,4), dpi=100)
ax = fig.add_subplot(111)
x = np.arange(25,156,1) # Create x values
#print(x)
#Using CDF of Beta distribution
y = beta.cdf(x,2.14750324,0.65953124, scale=130, loc=25)
print("45\u2103 CDF(%) \u03B1=2.14, \u03B2=0.65: ",np.c_[x, y*100])
#Plot CDF curve
plt.plot(x,y, color = 'blue',label='\u03B1=2.14, \u03B2=0.65', linewidth=1.75)
# Scatter points
A = [25, 45, 150, 155]
B = [0, 0.01, 0.8,1]
ax = fig.add_subplot(111)
# location of the scatter points
plt.annotate('(25,0)', xy=(25, 0), xytext=(20, .05))
plt.annotate('(45,0.01)', xy=(45, 0.01), xytext=(38, .055))
plt.annotate('(150,0.8)', xy=(150, 0.8), xytext=(128, .8))
plt.annotate('(155,1)', xy=(155, 1), xytext=(137, 0.98))
plt.xlabel('Temperature (\u2103)')
plt.ylabel('CDF (Motor Failure)')
plt.legend(fontsize = 'small', loc='upper left')
# plotting the points
#plt.scatter(A, B, marker='o', markerfacecolor='blue', markersize=12)
plt.scatter(A, B, label= "stars", color= "red", marker= "o", s=40)
# draw straight line
d=.50
ax.margins(x=0)
ax.hlines(d, xmin=10, xmax=161,linewidth=1, color='k')
plt.yticks(np.arange(0, 1.1, 0.1))
plt.show()
```

Plotting failure reference curve for vibration:

```
from scipy.stats import beta
import matplotlib.pyplot as plt
import numpy as np
fig= plt.figure(figsize=(6,4), dpi=100)
ax = fig.add_subplot(111)
x = np.arange(0,7.2,0.1) # Create x values
#print(x)
# Using CDF of Beta distribution
```

```

y = beta.cdf(x,3.58844012,1.19446306, scale=7.1, loc=0)
# Plot CDF curve
plt.plot(x,y, color = 'blue',label="\u03B1=3.59, \u03B2=1.19", linewidth=1.75)
# Scatter points
A = [0, 1.8, 6.5, 7.1]
B = [0, 0.01, 0.8,1]
ax = fig.add_subplot(111)
# location of the scatter points
plt.annotate('(0,0)', xy=(0, 0), xytext=(-.3, .05))
plt.annotate('(1.8, 0.01)', xy=(1.8, 0.01), xytext=(1.21, 0.05))
plt.annotate('(6.5, 0.8)', xy=(6.5, 0.8), xytext=(5.3, .78))
plt.annotate('(7.1, 1)', xy=(6.8, 1), xytext=(6.15, .98))
plt.xlabel('Vibration (mm/s)')
plt.ylabel('CDF (Fan Failure)')
plt.legend(fontsize = 'small')
# plotting the points
#plt.scatter(A, B, marker='o', markerfacecolor='blue', markersize=12)
plt.scatter(A, B, label= "stars", color= "red", marker= "o", s=40)
# draw straight line
d=.50
ax.margins(x=0)
ax.hlines(d, xmin=-.3, xmax=7.2,linewidth=1, color='k')
plt.yticks(np.arange(0, 1.1, 0.1))
plt.show()

```

Appendix C

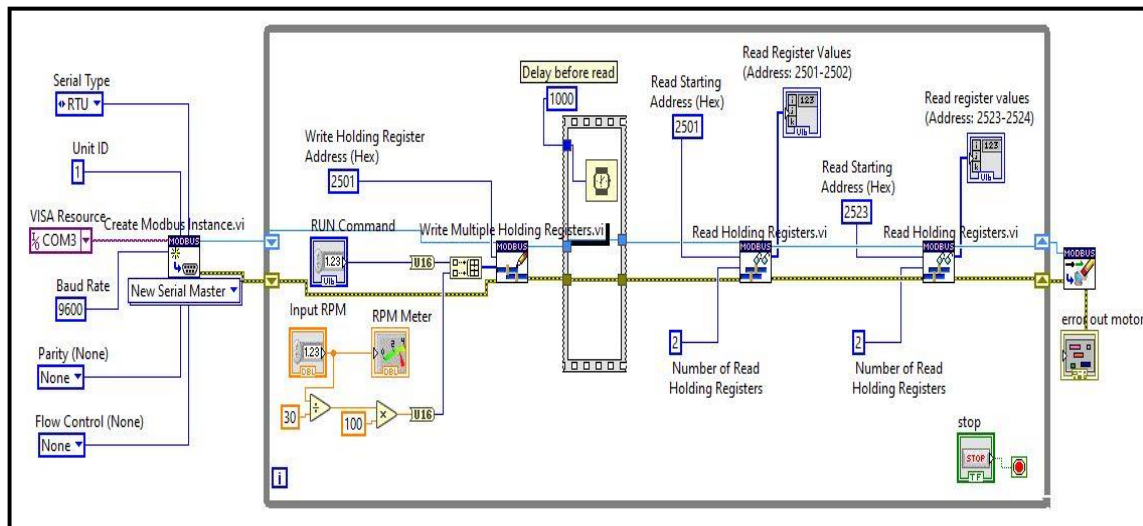
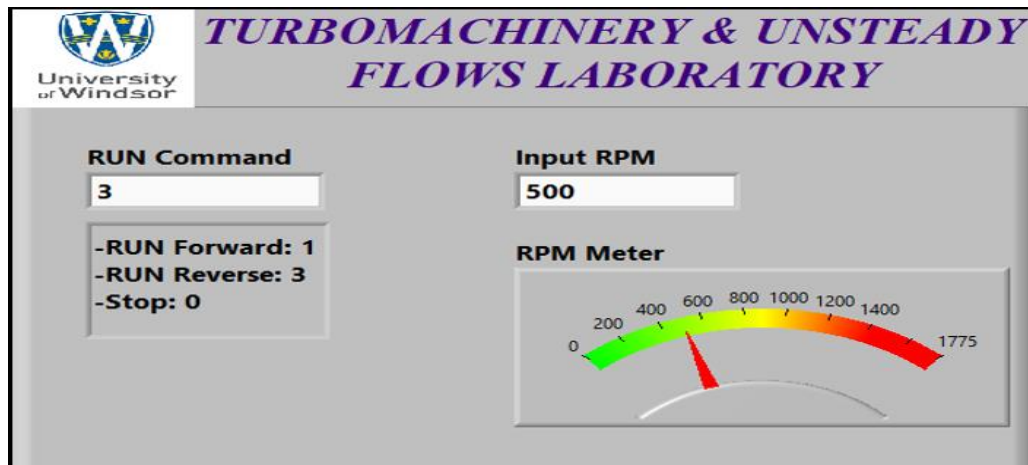
Alpha and Beta Values for Different Optimization Algorithms

Temperature					
Optimization Algorithm	Mean Squared Error Loss Function Value	Beta Distribution CDF Parameters			
		Alpha	Beta	Location	Scale
Nelder- mead	6.476e-13	2.14750324	0.65953124	25	130
TNC	1.184e-08	2.14030247	0.6588179	25	130
BFGS	4.786e-10	2.14903426	0.6596868	25	130
CG	9.128e-13	2.14762377	0.65954841	25	130
Powell	6.048e-07	2.14755403	0.6595388	25	130

Vibration					
Optimization Algorithm	Mean Squared Error Loss Function Value	Beta Distribution CDF Parameters			
		Alpha	Beta	Location	Scale
Nelder- mead	2.862e-13	3.58851886	1.19447976	0	7.1
TNC	2.779e-08	3.56659719	1.19061271	0	7.1
BFGS	5.748e-09	3.57854365	1.19275383	0	7.1
CG	2.488e-07	3.65752775	1.20655799	0	7.1
Powell	1.638e-33	3.58855558	1.19448419	0	7.1

Appendix D

Front Panel and Block Diagram of the Remote Motor Control Program Using LabView.



Vita Auctoris

NAME: Forhad Reza

PLACE OF BIRTH: Lakshmipur, Bangladesh

YEAR OF BIRTH: 1989

EDUCATION: M.A.Sc. in Mechanical Engineering
University of Windsor, Windsor, ON, 2020

B.A.Sc. in Electrical and Electronic Engineering
American International University-Bangladesh,
Dhaka, Bangladesh, 2011